

Overnight GARCH-Itô Volatility Models

Donggyu Kim^a, Minseok Shin^a, and Yazhen Wang^b

^aCollege of Business,

Korea Advanced Institute of Science and Technology (KAIST),

^bDepartment of Statistics, University of Wisconsin-Madison

June 20, 2022

Abstract

Various parametric volatility models for financial data have been developed to incorporate high-frequency realized volatilities and better capture market dynamics. However, because high-frequency trading data are not available during the close-to-open period, the volatility models often ignore volatility information over the close-to-open period and thus may suffer from loss of important information relevant to market dynamics. In this paper, to account for whole-day market dynamics, we propose an overnight volatility model based on Itô diffusions to accommodate two different instantaneous volatility processes for the open-to-close and close-to-open periods. We develop a weighted least squares method to estimate model parameters for two different periods and investigate its asymptotic properties. We conduct a simulation study to check the finite sample performance of the proposed model and method. Finally, we apply the proposed approaches to real trading data.

Keywords: high-frequency financial data, low-frequency financial data, quasi-maximum likelihood estimation, stochastic differential equation, volatility estimation and prediction

1 Introduction

Since Markowitz (1952) introduced the modern portfolio theory, measuring risk has become important in financial applications. Volatility itself is often employed as a proxy for risk. Furthermore, there are several risk measurements, such as Value at Risk (VaR), expected shortfall, and market beta (Duffie and Pan, 1997; Rockafellar and Uryasev, 2000; Sharpe, 1964). These risk measurements take volatilities as an important ingredient in their formulations, and their performances heavily depend on the accuracy of volatility estimation.

Generalized autoregressive conditional heteroskedasticity (GARCH) models are one of the most successful volatility models for low-frequency data (Bollerslev, 1986; Engle, 1982). They employ squared daily log-returns as innovations in conditional expected volatilities and are able to capture low-frequency market dynamics, such as volatility clustering and heavy tail. At the high-frequency level, nonparametric approaches, such as Itô processes and realized volatility estimators, are often utilized to model and estimate volatilities. Examples include two-time scale realized volatility (TSRV) (Zhang et al., 2005), multi-scale realized volatility (MSRV) (Zhang, 2006), kernel realized volatility (KRV) (Barndorff-Nielsen et al., 2008), quasi-maximum likelihood estimator (QMLE) (Aït-Sahalia et al., 2010; Xiu, 2010), pre-averaging realized volatility (PRV) (Jacod et al., 2009), and robust pre-averaging realized volatility (Fan and Kim, 2018). In practice, we often observe jumps in financial data, and the decomposition of daily variation into continuous and jump components can improve volatility estimation and aid with better explanation of volatility dynamics (Aït-Sahalia et al., 2012; Barndorff-Nielsen and Shephard, 2006; Corsi et al., 2010). For example, Fan and Wang (2007) and Zhang et al. (2016) employed the wavelet method to identify the jumps in given noisy high-frequency data. Mancini (2004) studied a threshold method for jump-detection and presented the order of an optimal threshold, and Jacod et al. (2009) introduced the jump robust pre-averaging realized (PRV) estimator. We call this realized volatility. There have been

several recent attempts to combine low-frequency GARCH and SV models and high-frequency realized volatilities. Examples include the realized volatility based modeling approaches (Andersen et al., 2003), the heterogeneous auto-regressive (HAR) models (Corsi, 2009), the high-frequency based volatility (HEAVY) models (Shephard and Sheppard, 2010), the realized GARCH models (Hansen et al., 2012), and the unified GARCH/SV-Itô models (Kim and Fan, 2019; Kim and Wang, 2016; Song et al., 2020). The realized volatility based models, such as HAR, HEAVY, and realized GARCH models, take reduced ARFIMA forms to model and forecast realized volatilities estimated from high-frequency data, and the unified GARCH/SV-Itô models provide theoretical platform to reconcile low-frequency GARCH/SV volatility representations and high-frequency volatility processes and harnesses realized volatilities and GARCH/SV models to yield better, albeit more complicated, modeling and inference for combining low- and high-frequency data. Empirical studies have shown that, with realized volatility as a part of the innovation, volatility models can better capture market dynamics. However, because high-frequency data are usually available only during trading hours, such as the open-to-close period, the high-frequency volatility models often include open-to-close integrated volatility in the innovation and ignore the overnight risk (Corsi, 2009; Kim and Wang, 2016; Song et al., 2020). Taylor (2007) showed that the overnight information is important for evaluating risk management models, so the volatility measured by the open-to-close high-frequency observations may significantly undervalue their risk. Furthermore, the overnight risk is often severe—for example, during the European debt crisis, Asian financial crisis, and so on—and so it is an important factor that accounts for market dynamics. From this point of view, there are several studies on the impact of overnight returns on volatility and modeling the volatility process using overnight returns and realized volatility. Hansen and Lunde (2005) studied optimal incorporation of the overnight information and proposed inverse weighting of the realized volatility and squared overnight returns by using the corresponding variance estimates. Andersen et al. (2011) modeled the overnight returns using an augmented GARCH type structure.

See also Martens (2002); Todorova and Souček (2014); Tseng et al. (2012) for more information on the impact of overnight volatility. These studies document an increasing interest in developing Itô process-based models that provide a rigorous mathematical formulation for using both open-to-close high-frequency data and close-to-open low-frequency data to analyze whole-day market dynamics.

In this paper, we develop an instantaneous volatility model for a whole-day period. The whole-day is broken down into two time periods, the open-to-close and close-to-open periods. During the open-to-close period, we observe high-frequency trading data, whereas during the close-to-open period, we observe low-frequency close and open prices. To reflect this structural difference, we develop two different instantaneous volatility processes for the open-to-close and close-to-open periods. For example, for the open-to-close period, we use the current integrated volatility as an innovation to reflect the market dynamics immediately, which helps to adapt to the rapid change in the volatility process, as occurs in the high-frequency volatility models (Corsi, 2009; Hansen et al., 2012; Shephard and Sheppard, 2010; Song et al., 2020). For the close-to-open period, we employ the current squared log-return as an innovation, which brings us back to the discrete-time GARCH model for the close-to-open period. The proposed structure implies that the conditional expected volatility for the whole-day period is a function of past open-to-close integrated volatilities and squared close-to-open log-returns. We call this volatility model the overnight GARCH-Itô (OGI) model. Moreover, to estimate its model parameters, we develop a quasi-likelihood estimation procedure. Specifically, for the open-to-close period, we employ realized volatilities as a proxy for the corresponding conditional expected volatilities, whereas for the close-to-open period, we adopt squared close-to-open log-returns as a proxy for the corresponding conditional expected volatilities. These proxies have heterogeneous variances that are related to the accuracy of the proxies. To reflect this, we calculate their variances and assign different weights to each proxy. As a result, the proposed estimation method takes the form of weighted least squares. We apply the

overnight GARCH-Itô model for a VaR study.

The rest of this paper is organized as follows. Section 2 introduces the overnight GARCH-Itô model and discusses its properties. Section 3 proposes weighted least squares estimation methods and investigates its asymptotic properties. Section 4 conducts a simulation study to check the finite sample performance of the proposed estimation methods. Section 5 applies the proposed overnight GARCH-Itô model and method to real trading data. The conclusion is presented in Section 6. We collect the proofs in the Supplement document.

2 Overnight GARCH-Itô models

In this section, we develop an Itô diffusion process to capture the whole-day market dynamics. To separate the parameters for the high-frequency period (open-to-close) and low-frequency period (close-to-open), we use the subscript or superscript H and L , respectively. For the low-frequency GARCH volatility related parameter, we use superscript g .

Definition 1. We call the log-price X_t an overnight GARCH-Itô (OGI) process if it satisfies

$$dX_t = \mu_t dt + \sigma_t(\theta) dB_t + J_t d\Lambda_t,$$

$$\sigma_t^2(\theta) = \begin{cases} \sigma_{[t]}^2(\theta) + \frac{(t-[t])^2}{\lambda^2}(\omega_{H1} + \gamma_H \sigma_{[t]}^2(\theta)) - \frac{t-[t]}{\lambda}(\omega_{H2} + \sigma_{[t]}^2(\theta)) \\ + \frac{\beta_H(t-[t])([t]+\lambda-t)}{\lambda^2(1-\lambda)} \sum_{j=1}^{\infty} \gamma^{j-1} \left(\int_{[t]+\lambda-j}^{[t]+1-j} \sigma_s(\theta) dB_s \right)^2 \\ + \frac{\alpha_H}{\lambda} \int_{[t]}^t \sigma_s^2(\theta) ds + \frac{\nu_H}{\lambda^2} ([t] + \lambda - t) (Z_t^H)^2, & \text{if } t \in ([t], [t] + \lambda], \\ \sigma_{[t]+\lambda}^2(\theta) + \frac{t-[t]-\lambda}{1-\lambda}(\omega_L + (\gamma_L - 1)\sigma_{[t]+\lambda}^2(\theta)) \\ + \frac{\alpha_L(t-[t]-\lambda)([t]+1-t)}{(1-\lambda)^2\lambda} \sum_{j=1}^{\infty} \gamma^{j-1} \int_{[t]+1-j}^{[t]+1-j+\lambda} \sigma_s^2(\theta) ds \\ + \frac{\beta_L}{1-\lambda} \left(\int_{[t]+\lambda}^t \sigma_s(\theta) dB_s \right)^2 + \frac{\nu_L}{(1-\lambda)^2} ([t] + 1 - t) (Z_t^L)^2, & \text{if } t \in ([t] + \lambda, [t] + 1], \end{cases}$$

where $[t]$ denotes the integer part of t except that $[t] = t - 1$ when t is an integer, λ is the time length

of the trading period, $Z_t^H = \int_{[t]}^t dW_s$, $Z_t^L = \int_{\lambda+[t]}^t dW_s$, $\gamma = \gamma_H \gamma_L$, and $\theta = (\omega_{H1}, \omega_{H2}, \omega_L, \gamma_H, \gamma_L, \alpha_H, \alpha_L, \beta_H, \beta_L, \nu_H, \nu_L)$ is the model parameters. For the jump part, Λ_t is the Poisson process with constant intensity μ_J , and the jump sizes J_t 's are independent of the continuous diffusion processes. Furthermore, the jump size J_t is equal to zero for the overnight period.

The instantaneous volatility process of the OGI model is continuous with respect to time. That is, its trajectories are continuous. For the open-to-close period—for example, $[t] \leq t \leq [t] + \lambda$ —the instantaneous volatility process reflects the market risk via the current integrated volatility and past squared overnight returns, whereas for the close-to-open period, $[t] + \lambda \leq t \leq [t] + 1$, the instantaneous volatility process utilizes the current log-return and past open-to-close integrated volatilities to express the market risk. Specifically, the past risk factors are calculated through exponentially weighted averages with γ order. Furthermore, to account for the U-shape pattern of the intra-day volatility process (Andersen et al., 2019), the instantaneous volatility process has the quadratic terms with respect to time t . Thus, with appropriate choices of ω_{H1} and ω_{H2} , the OGI model can explain the U-shape pattern. At the market open time, the instantaneous volatility process has the following GARCH structure:

$$\begin{aligned} \sigma_n^2(\theta) &= \omega_L + \gamma_L(\omega_{H1} - \omega_{H2}) + \gamma \sigma_{n-1}^2(\theta) + \frac{\gamma_L \alpha_H}{\lambda} \int_{n-1}^{n-1+\lambda} \sigma_t^2(\theta) dt \\ &\quad + \frac{\beta_L}{1-\lambda} (X_n - X_{n-1+\lambda} - \int_{n-1+\lambda}^n \mu_t dt)^2, \end{aligned}$$

where n is an integer, and at the market close time,

$$\begin{aligned} \sigma_{n+\lambda}^2(\theta) &= \omega_{H1} - \omega_{H2} + \gamma_H \omega_L + \gamma \sigma_{n-1+\lambda}^2(\theta) + \frac{\alpha_H}{\lambda} \int_n^{n+\lambda} \sigma_t^2(\theta) dt \\ &\quad + \frac{\gamma_H \beta_L}{1-\lambda} (X_n - X_{n-1+\lambda} - \int_{n-1+\lambda}^n \mu_t dt)^2. \end{aligned} \tag{2.1}$$

Thus, the instantaneous volatility process is some quadratic interpolation of the GARCH volatility

with the open-to-close integrated volatility and squared close-to-open log-return as the innovation. To account for the random fluctuations of the instantaneous volatilities, we introduce Z_t^H and Z_t^L with the scale parameters ν_H and ν_L . When considering only one of the open-to-close and close-to-open periods and ignoring the other period, the OGI model recovers the realized GARCH-Itô process (Hansen et al., 2012; Song et al., 2020) or unified GARCH-Itô process (Kim and Wang, 2016). Thus, unlike the proposed OGI model, these models only incorporate one innovation term of the integrated volatility and squared log-return in their conditional volatility.

Because our main interest lies in measuring the whole-day risk, to estimate the model parameters, we use nonparametric integrated volatility estimators (Barndorff-Nielsen et al., 2008; Jacod et al., 2009; Zhang, 2006) and squared log-returns as proxies for the parametric conditional expected integrated volatility. Thus, it is important to investigate properties of the integrated volatility of the proposed OGI model. The following theorem shows the properties of integrated volatilities.

Theorem 1. *For the OGI model, we have the following properties.*

(a) *The integrated volatilities have the following structure. For $0 < \alpha_H < 1$, $0 < \beta_L < 1$, and $n \in \mathbb{N}$, we have*

$$\int_{n-1}^n \sigma_t^2(\theta) dt = h_n(\theta) + D_n \quad a.s., \quad (2.2)$$

$$\int_{n-1}^{n-1+\lambda} \sigma_t^2(\theta) dt = \lambda h_n^H(\theta) + D_n^H \quad a.s., \quad (2.3)$$

$$\int_{n-1+\lambda}^n \sigma_t^2(\theta) dt = (1 - \lambda) h_n^L(\theta) + D_n^L \quad a.s., \quad (2.4)$$

where

$$h_n(\theta) = \omega^g + \gamma h_{n-1}(\theta) + \frac{\alpha^g}{\lambda} \int_{n-2}^{n-2+\lambda} \sigma_t^2(\theta) dt + \frac{\beta^g}{1 - \lambda} (X_{n-1} - X_{n-2+\lambda} - \int_{n-2+\lambda}^{n-1} \mu_t dt)^2,$$

$$h_n^H(\theta) = \omega_H^g + \gamma h_{n-1}^H(\theta) + \frac{\alpha_H^g}{\lambda} \int_{n-2}^{n-2+\lambda} \sigma_t^2(\theta) dt + \frac{\beta_H^g}{1 - \lambda} (X_{n-1} - X_{n-2+\lambda} - \int_{n-2+\lambda}^{n-1} \mu_t dt)^2,$$

$$h_n^L(\theta) = \omega_L^g + \gamma h_{n-1}^L(\theta) + \frac{\alpha_L^g}{\lambda} \int_{n-2}^{n-2+\lambda} \sigma_t^2(\theta) dt + \frac{\beta_L^g}{1-\lambda} (X_{n-1} - X_{n-2+\lambda} - \int_{n-2+\lambda}^{n-1} \mu_t dt)^2,$$

D_n, D_n^H, D_n^L are martingale differences and $\omega^g, \gamma, \alpha^g, \beta^g, \omega_H^g, \alpha_H^g, \beta_H^g, \omega_L^g, \alpha_L^g, \beta_L^g$ are functions of θ . Their detailed forms are defined in Theorem ?? in the supplement document.

(b) We have

$$\begin{aligned} E \left[(D_n^H)^2 \middle| \mathcal{F}_{n-1} \right] &= \varphi_n^H(\theta) = \lambda^2 \nu_H^g \text{ a.s.}, \\ E \left[(D_n^{LL})^2 \middle| \mathcal{F}_{n-1} \right] &= \varphi_n^L(\theta) \\ &= F_{\beta_L,1} s_{n-1}^4(\theta) + F_{\beta_L,2} \omega_L s_{n-1}^2(\theta) + F_{\beta_L,3} \omega_L^2 + (1-\lambda)^2 \nu_L^g \text{ a.s.}, \end{aligned}$$

where $D_n^{LL} = D_n^L + 2 \int_{\lambda+n-1}^n (X_t - X_{\lambda+n-1}) \sigma_t(\theta_0) dB_t$, ν_H^g and ν_L^g are defined in (??) and (??), respectively, $s_{n-1}^2(\theta)$ is defined in (??), and $F_{\beta_L,i}$'s are functions of β_L defined in (??) in the supplement document.

Theorem 1 (a) shows that the integrated volatility can be decomposed into the GARCH volatility and martingale difference. This structure implies that the daily conditional expected volatility is a function of the past open-to-close integrated volatilities and squared close-to-open log-returns. That is, under the OGI process, the market dynamics can be explained by the open-to-close integrated volatility and squared close-to-open log-returns, which represent volatilities for the open-to-close and close-to-open periods, respectively. Thanks to these two different volatility sources, we expect the proposed OGI model to capture the market dynamics well. In the empirical study, we find that the integrated volatilities and squared log-returns help to account for the market dynamics (see Section 5).

Remark 1. Based on the result of Theorem 1, we can predict the one period ahead volatility. In practice, we often need to predict the multi-period ahead volatility. To do this, we use the following

relationship:

$$\begin{aligned}
E \left[\int_{n-1}^n \sigma_t^2(\theta) dt \middle| \mathcal{F}_{n-2} \right] &= E \left[E \left[\int_{n-1}^n \sigma_t^2(\theta) dt \middle| \mathcal{F}_{n-1} \right] \middle| \mathcal{F}_{n-2} \right] \\
&= E [h_n(\theta) | \mathcal{F}_{n-2}] \\
&= \omega^g + \gamma h_{n-1}(\theta) + \alpha^g h_{n-1}^H(\theta) + \beta^g h_{n-1}^L(\theta) \text{ a.s.}
\end{aligned}$$

Then, recursively, we can obtain the multi-period prediction.

As we discussed above, we estimate the model parameters via the relationship between the conditional GARCH volatilities, $h_n^H(\theta)$, $h_n^L(\theta)$, and $h_n(\theta)$, and the corresponding integrated volatility or squared log-return. Thus, to study the low-frequency volatility dynamics, we only need Theorem 1 (a). That is, under the model assumptions (2.2)–(2.4), we develop the rest of the paper. In comparison with direct volatility modeling based on realized volatility such as HAR, HEAVY, and realized GARCH models (Andersen et al., 2003; Corsi, 2009; Hansen et al., 2012; Shephard and Sheppard, 2010), the unified GARCH-Itô model and OGI model may be more difficult or even less practical for drawing statistical inferences from combined low- and high-frequency data. However, like the unified GARCH-Itô model case, the OGI approach indicates the existence of the diffusion process, which satisfies the conditions (2.2)–(2.4) and fills the gap between the low-frequency discrete time series volatility modeling and the high-frequency continuous time diffusion process. Because the purpose of this paper is to develop diffusion processes that can account for the low-frequency market dynamics, the parameter of interest is the GARCH parameter $\theta^g = (\omega_H^g, \omega_L^g, \gamma, \alpha_H^g, \alpha_L^g, \beta_H^g, \beta_L^g)$. We notice that, under the model assumption, we need the common γ condition for the open-to-close and close-to-open conditional volatilities to have the GARCH conditional volatility form for $h_n^H(\theta)$, $h_n^L(\theta)$, and $h_n(\theta)$. When it comes to estimating GARCH parameters, we assume that the open-to-close and close-to-open volatilities have different dynamic structures, so we make inferences for $h_n^H(\theta)$ and $h_n^L(\theta)$ separately under the common γ condition. Details can be found in Section 3.

3 Estimation procedure

3.1 A model setup

We assume that the underlying diffusion process follows the OGI process defined in Definition 1. The high-frequency observations during the d th open-to-close period are observed at $t_{d,i}, i = 1, \dots, m_d$, where $d - 1 = t_{d,0} < t_{d,1} < \dots < t_{d,m_d} = \lambda + d - 1$. Let m be the average number of the high-frequency observations, that is, $m = \frac{1}{n} \sum_{d=1}^n m_d$. Due to market inefficiencies, such as the bid-ask spread, asymmetric information, and so on, the high-frequency data are masked by the microstructure noise. To account for this, we assume that the observed log-prices during the open-to-close period have the following additive noise structure:

$$Y_{t_{d,i}} = X_{t_{d,i}} + \epsilon_{t_{d,i}}, \quad \text{for } d = 1, \dots, n, i = 1, \dots, m_d - 1,$$

where X_t is the true log-price, $\epsilon_{t_{d,i}}$ is microstructure noise with mean zero and variance η_d , and the log-price and microstructure noise are independent. The effect of μ_t is negligible regarding high-frequency realized volatility estimators, and the magnitude of daily returns is relatively small. Thus, for simplicity, we assume $\mu_t = 0$ in Definition 1. We note that the theoretical results in Theorem 2 can be established in the similar way with non-zero μ_t under some piecewise constant condition for μ_t . In contrast, during the close-to-open period, we only observe the low-frequency observations, open and close prices. In the low-frequency time series modeling, we often assume that the true low-frequency prices are observed. In practice, the microstructure noise may exist in the low-frequency observations, but its impact on the low-frequency modeling is relatively small. Thus, we also assume that the true low-frequency observations, the open and close prices X_d and $X_{\lambda+d}$, are observed at the open and close times, $t_{d+1,0}$ and $t_{d+1,m_{d+1}}$.

Remark 2. For the microstructure noise, we may need a stationary condition to estimate the

integrated volatility with the optimal convergence rate $m^{-1/4}$ (Barndorff-Nielsen et al., 2008; Fan and Kim, 2018; Jacod et al., 2009; Kim et al., 2016; Zhang, 2006). For example, we may impose a ARMA-type structure on the microstructure noise and assume some dependence between the price processes and the microstructure noise. However, in this paper, we directly adopt a well-performing nonparametric realized volatility estimator, which can be obtained under certain structures of the microstructure without affecting the volatility modeling. Thus, we can put such structures on the microstructure noise, as long as we can secure the well-performing realized volatility estimator.

3.2 GARCH parameters estimation

We first fix some notations. For any given vector $b = (b_i)_{i=1,\dots,k}$, we define $\|b\|_{\max} = \max_i |b_i|$. Let C 's be positive generic constants whose values are independent of θ , n , and m and may change from occurrence to occurrence. In this section, we develop an estimation procedure for the GARCH parameters, $\theta^g = (\omega_H^g, \omega_L^g, \gamma, \alpha_H^g, \alpha_L^g, \beta_H^g, \beta_L^g)$, which are minimum required parameters to evaluate the GARCH volatilities defined in Theorem 1, where elements of θ^g are defined in Theorem ?? in the supplement document. We denote the true GARCH parameter by $\theta_0^g = (\omega_{H,0}^g, \omega_{L,0}^g, \gamma_0, \alpha_{H,0}^g, \alpha_{L,0}^g, \beta_{H,0}^g, \beta_{L,0}^g)$.

Theorem 1 indicates that integrated volatilities can be decomposed into the GARCH volatility terms $h_n^H(\theta_0^g)$ and $h_n^L(\theta_0^g)$, and the martingale difference terms D_n^H and D_n^L . This fact inspires us to use the integrated volatilities as proxies of the GARCH volatilities. Then, as the sample period goes to infinity, the martingale convergence theorem may provide consistency of the estimators. However, the integrated volatilities are not observable, so we first need to estimate them. For the open-to-close period, we use the high-frequency observations to estimate the open-to-close integrated volatility nonparametrically (Aït-Sahalia et al., 2012; Barndorff-Nielsen et al., 2008; Corsi et al., 2010; Fan and Wang, 2007; Jacod et al., 2009; Xiu, 2010; Zhang, 2006; Zhang et al., 2016), and we call these nonparametric estimators “realized volatility.” Under mild conditions, we

can show that realized volatility converges to integrated volatility with the optimal convergence rate $m^{-1/4}$ (Barndorff-Nielsen et al., 2008; Jacod et al., 2009; Kim et al., 2016; Tao et al., 2013; Xiu, 2010; Zhang, 2006). In the numerical study, we employ the jump robust pre-averaging realized (PRV) estimator (Aït-Sahalia and Xiu, 2016; Jacod et al., 2009). However, for the close-to-open period, high-frequency data are not available, so we use the squared close-to-open return as the proxy. Note that Itô's lemma indicates

$$(X_n - X_{\lambda+n-1})^2 = \int_{\lambda+n-1}^n \sigma_t^2(\theta_0) dt + 2 \int_{\lambda+n-1}^n (X_t - X_{\lambda+n-1}) \sigma_t(\theta_0) dB_t \text{ a.s.}$$

This implies that the squared close-to-open return can also be decomposed into the GARCH volatility and martingale difference. That is, we have the following relationships:

$$\begin{aligned} \int_{n-1}^{\lambda+n-1} \sigma_t^2(\theta_0) dt &= \lambda h_n^H(\theta_0^g) + D_n^H \text{ a.s.}, \\ (X_n - X_{\lambda+n-1})^2 &= (1 - \lambda) h_n^L(\theta_0^g) + D_n^{LL} \text{ a.s.}, \end{aligned}$$

where $D_n^{LL} = D_n^L + 2 \int_{\lambda+n-1}^n (X_t - X_{\lambda+n-1}) \sigma_t(\theta_0) dB_t$. We use the above relationships to estimate the GARCH parameter θ_0^g .

The variances of the martingale differences D_n^H and D_n^{LL} indicate the accuracy of the GARCH volatility information coming from the proxies $\int_{n-1}^{\lambda+n-1} \sigma_t^2(\theta_0) dt$ and $(X_n - X_{\lambda+n-1})^2$, so each proxy with the smaller variance is closer to the corresponding GARCH volatility. Thus, as we incorporate the variance information into an estimation procedure, we expect to improve its performance. For example, we can standardize the proxies as follows:

$$\frac{\left(\int_{n-1}^{\lambda+n-1} \sigma_t^2(\theta_0) dt - \lambda h_n^H(\theta_0^g) \right)^2}{E \left[(D_n^H)^2 \right]} \quad \text{and} \quad \frac{\left((X_n - X_{\lambda+n-1})^2 - (1 - \lambda) h_n^L(\theta_0^g) \right)^2}{E \left[(D_n^{LL})^2 \right]}.$$

The unit expectations help to assign a larger weight to a more accurate proxy. In the empirical

study, we find that the variance of the integrated volatilities is smaller than that of the squared close-to-open returns. That is, the open-to-close proxy is more accurate, so we make more use of the information from the open-to-close period by assigning to it a larger weight. To compare the proxies and GARCH volatilities, we employ the weighted least squares estimation as follows:

$$L_n(\theta^g) = -\frac{1}{n} \sum_{i=1}^n \left[\frac{(IV_i - \lambda h_i^H(\theta^g))^2}{\hat{\phi}_H} + \frac{((X_i - X_{\lambda+i-1})^2 - (1-\lambda)h_i^L(\theta^g))^2}{\hat{\phi}_L} \right],$$

where the GARCH volatility terms $h_i^H(\theta^g)$ and $h_i^L(\theta^g)$ are defined in Theorem 1, $IV_i = \int_{i-1}^{\lambda+i-1} \sigma_t^2(\theta_0) dt$, and $\hat{\phi}_H$ and $\hat{\phi}_L$ are consistent estimators of variances of martingale differences D_n^H and D_n^{LL} , respectively. To evaluate the above quasi-likelihood function, we first need to estimate the integrated volatility IV_i . It can be estimated by the realized volatility estimator, which is denoted by RV_i . Then we estimate the GARCH volatilities as follows:

$$\hat{h}_n^H(\theta^g) = \omega_H^g + \gamma \hat{h}_{n-1}^H(\theta^g) + \frac{\alpha_H^g}{\lambda} RV_{n-1} + \frac{\beta_H^g}{1-\lambda} (X_{n-1} - X_{\lambda+n-2})^2, \quad (3.1)$$

$$\hat{h}_n^L(\theta^g) = \omega_L^g + \gamma \hat{h}_{n-1}^L(\theta^g) + \frac{\alpha_L^g}{\lambda} RV_{n-1} + \frac{\beta_L^g}{1-\lambda} (X_{n-1} - X_{\lambda+n-2})^2. \quad (3.2)$$

We note that the conditional expected volatilities for the open-to-close and close-to-open periods have the common γ as in (3.1) and (3.2), which makes it possible to have the GARCH form for the whole-day conditional expected volatility. To evaluate the GARCH volatilities, we use RV_1 and the sample variance of the close-to-open log-returns as the initial values $h_0^H(\theta^g)$ and $h_0^L(\theta^g)$, respectively. The effect of the initial value has the negligible order n^{-1} (see Lemma 1 in Kim and Wang (2016)), so its choice does not significantly affect the parameter estimation. With these estimators, we define the quasi-likelihood function as follows:

$$\hat{L}_{n,m}(\theta^g) = -\frac{1}{n} \sum_{i=1}^n \left[\frac{(RV_i - \lambda \hat{h}_i^H(\theta^g))^2}{\hat{\phi}_H} + \frac{((X_i - X_{\lambda+i-1})^2 - (1-\lambda) \hat{h}_i^L(\theta^g))^2}{\hat{\phi}_L} \right], \quad (3.3)$$

and we obtain the estimator of the GARCH parameters θ_0^g by maximizing the quasi-likelihood function. That is,

$$\hat{\theta}^g = \arg \max_{\theta^g \in \Theta^g} \hat{L}_{n,m}(\theta^g),$$

where Θ^g is the parameter space of θ^g . We call the estimator the weighted least squares estimator (WLSE). To obtain the variances of martingale differences, $\hat{\phi}_H$ and $\hat{\phi}_L$, we employ the QMLE method as follows. We define the quasi-likelihood functions for the open-to-close and close-to-open, respectively, in the following manner:

$$\hat{L}_{n,m}^H(\theta_H^g) = -\frac{1}{n} \sum_{i=1}^n \left[\log(\lambda \hat{h}_i^H(\theta_H^g)) + \frac{RV_i}{\lambda \hat{h}_i^H(\theta_H^g)} \right], \quad (3.4)$$

$$\hat{L}_{n,m}^L(\theta_L^g) = -\frac{1}{n} \sum_{i=1}^n \left[\log((1-\lambda) \hat{h}_i^L(\theta_L^g)) + \frac{(X_i - X_{\lambda+i-1})^2}{(1-\lambda) \hat{h}_i^L(\theta_L^g)} \right], \quad (3.5)$$

where $\theta_H^g = (\omega_H^g, \gamma, \alpha_H^g, \beta_H^g)$ and $\theta_L^g = (\omega_L^g, \gamma, \alpha_L^g, \beta_L^g)$. Then we find their maximizers, which are denoted by $\hat{\theta}_H^g$ and $\hat{\theta}_L^g$. Using the residuals, we estimate the variances of martingale difference in the following way:

$$\begin{aligned} \hat{\phi}_H &= \frac{1}{n} \sum_{i=1}^n (RV_i - \lambda \hat{h}_i^H(\hat{\theta}_H^g))^2, \\ \hat{\phi}_L &= \frac{1}{n} \sum_{i=1}^n ((X_i - X_{\lambda+i-1})^2 - (1-\lambda) \hat{h}_i^L(\hat{\theta}_L^g))^2. \end{aligned}$$

Similar to the proofs of Theorems 3 and 5 in Kim and Wang (2016), we can establish their consistency.

Remark 3. There are other possible choices of the variance of the martingale differences. For example, we can use the conditional variances in Theorem 1 (b) to evaluate the quasi-likelihood function (3.3). However, the conditional variance heavily depends on the underline OGI process, which may cause some bias when the underline model is misspecified. Thus, to make robust

inferences, we use the unconditional variance instead of the conditional variance. Furthermore, the proposed procedure has a more simple structure, which may help to reduce estimation errors. We note that the proposed two-step weighted least square estimation procedure works well as long as the first-step variance estimators are consistent. Thus, we can easily incorporate the other variance estimator. According to our empirical analysis, the unconditional variance estimator provides more stable results than the conditional variance estimator. Thus, we use the unconditional variance and only report its related results. If we can estimate conditional variance in a robust way, it may show better performance. However, obtaining the robustness is not straightforward because we need to impose structure on the process to evaluate the conditional variance. We leave this for a future study.

To establish asymptotic properties for the proposed WLSE, we need the following technical assumptions.

Assumption 1.

(1) $\theta_0^g \in \Theta^g = \{(\omega_H^g, \omega_L^g, \gamma, \alpha_H^g, \alpha_L^g, \beta_H^g, \beta_L^g); \omega_l < \omega_H^g, \omega_L^g < \omega_u, \gamma_l < \gamma < \gamma_u < 1, \alpha_l < \alpha_H^g, \alpha_L^g < \alpha_u, \beta_l < \beta_H^g, \beta_L^g < \beta_u < 1, \|\mathbf{A}\|_2 < 1\}$, where $\omega_l, \omega_u, \gamma_l, \gamma_u, \alpha_l, \alpha_u, \beta_l, \beta_u$ are some known positive constants, $\|\cdot\|_2$ is the matrix spectral norm, and $\mathbf{A} = \begin{pmatrix} \gamma + \frac{\alpha_H^g}{\lambda} & \frac{\beta_H^g}{1-\lambda} \\ \frac{\alpha_L^g}{\lambda} & \gamma + \frac{\beta_L^g}{1-\lambda} \end{pmatrix}$.

(2) We have for some positive constant C ,

$$\sup_d E [(X_{\lambda+d-1} - X_{d-1})^4] \leq C, \quad \sup_d E [(X_d - X_{\lambda+d-1})^4] \leq C, \quad \sup_d E [(D_d^{LL})^4] \leq C.$$

(3) We have $C_1 m \leq m_d \leq C_2 m$ for all d , and $\max_d \sup_{1 \leq j \leq m_d} |t_{d,j} - t_{d,j-1}| = O(m^{-1})$.

(4) For any $d \in \mathbb{N}$, $E(|RV_d - IV_d|^2) \leq Cm^{-1/2}$.

(5) (D_d^H, D_d^{LL}) is a stationary process.

(6) $|\widehat{\phi}_H - \phi_{H0}| = o_p(1)$ and $|\widehat{\phi}_L - \phi_{L0}| = o_p(1)$, where $\phi_{H0} = E \left[(D_n^H)^2 \right]$ and $\phi_{L0} = E \left[(D_n^{LL})^2 \right]$.

Remark 4. Assumption 1(2) is about the finite 4th moment condition, which is the minimum requirement when handling the second moment target parameter. Under some finite 4th moment conditions, Assumption 1(4) is satisfied (Kim et al., 2018; Tao et al., 2013). However, when there is a jump part in the diffusion process, this condition may be violated. In this case, we need to employ some jump robust realized volatility (Ait-Sahalia and Xiu, 2016; Zhang et al., 2016) and derive some uniform convergence with respect to time d . Finally, Assumption 1(5) is required to derive an asymptotic normal distribution of the proposed WLSE.

The following theorem investigates the asymptotic behaviors of the proposed WLSE $\widehat{\theta}$.

Theorem 2. *Under Assumption 1, we have*

$$\|\widehat{\theta}^g - \theta_0^g\|_{\max} = O_p(m^{-1/4} + n^{-1/2}). \quad (3.6)$$

Furthermore, we suppose that $nm^{-1/2} \rightarrow 0$ as $m, n \rightarrow \infty$. Then we have

$$\sqrt{n}(\widehat{\theta}^g - \theta_0^g) \xrightarrow{d} N(0, A^{-1}BA^{-1}), \quad (3.7)$$

where

$$A = E \left[\frac{\lambda^2}{\phi_{H0}} \frac{\partial h_1^H(\theta^g)}{\partial \theta^g} \frac{\partial h_1^H(\theta^g)}{\partial \theta^{g\top}} \Big|_{\theta^g = \theta_0^g} + \frac{(1-\lambda)^2}{\phi_{L0}} \frac{\partial h_1^L(\theta^g)}{\partial \theta^g} \frac{\partial h_1^L(\theta^g)}{\partial \theta^{g\top}} \Big|_{\theta^g = \theta_0^g} \right],$$

$$B = E \left[\frac{\lambda^2 \varphi_1^H(\theta_0)}{\phi_{H0}^2} \frac{\partial h_1^H(\theta^g)}{\partial \theta^g} \frac{\partial h_1^H(\theta^g)}{\partial \theta^{g\top}} \Big|_{\theta^g = \theta_0^g} + \frac{(1-\lambda)^2 \varphi_1^L(\theta_0)}{\phi_{L0}^2} \frac{\partial h_1^L(\theta^g)}{\partial \theta^g} \frac{\partial h_1^L(\theta^g)}{\partial \theta^{g\top}} \Big|_{\theta^g = \theta_0^g} \right],$$

$\varphi_i^H(\theta_0)$ and $\varphi_i^L(\theta_0)$ are defined in Theorem 1(b).

Remark 5. Theorem 2 shows that the WLSE $\widehat{\theta}^g$ has the convergence rate $m^{-1/4} + n^{-1/2}$. The first term, $m^{-1/4}$, comes from estimating the integrated volatility, which is known as the optimal

convergence rate in the case of high-frequency data with the presence of the microstructure noise. The second term, $n^{-1/2}$, is the usual convergence rate in the low-frequency data case. Under the stationary assumption, we also derive the asymptotic normality.

Remark 6. To derive the asymptotic normality, we need the condition $nm^{-1/2} \rightarrow 0$, which is too restrictive for the long sample period. If this condition is violated, the asymptotic normality may depend on $m^{1/4}(RV_d - IV_d)$, which is the quantity related to high-frequency estimation. If this term is some martingale difference, we may be able to relax the condition such as $nm^{-1} \rightarrow 0$. In this case, usually, m is huge, so it is not restrictive.

One of our objectives in this paper is to predict future volatility. The best predictor given the current available information \mathcal{F}_n is the conditional expected volatility—that is, the GARCH volatility $h_{n+1}(\theta_0^g)$. With the model parameter estimator, we estimate the GARCH volatility as follows:

$$\widehat{h}_{n+1}(\widehat{\theta}^g) = \widehat{\omega}^g + \widehat{\gamma}\widehat{h}_n(\widehat{\theta}^g) + \widehat{\alpha}^g\lambda^{-1}RV_n + \widehat{\beta}^g(1 - \lambda)^{-1}(X_n - X_{\lambda+n-1})^2,$$

where the GARCH parameters $\widehat{\omega}^g$, $\widehat{\alpha}^g$, and $\widehat{\beta}^g$ are estimated using the plug-in method with the WLSE $\widehat{\theta}^g$. The following corollary provides the consistency of the GARCH volatility estimator.

Corollary 1. *Under the assumptions of Theorem 2 (except for $nm^{-1/2} \rightarrow 0$), we have*

$$|\widehat{h}_{n+1}(\widehat{\theta}^g) - h_{n+1}(\theta_0^g)| = O_p(n^{-1/2} + m^{-1/4}).$$

3.3 Hypothesis tests

In financial practices, we are interested in the GARCH parameters $(\omega^g, \gamma, \alpha^g, \beta^g)$ and often make statistical inferences about them, such as hypothesis tests. In this section, we discuss how to conduct hypothesis tests for the GARCH parameters.

We first derive the asymptotic distribution of the GARCH parameter estimators. Theorem 2 implies that

$$\sqrt{n}(\hat{\theta}^g - \theta_0^g) \xrightarrow{d} N(0, A^{-1}BA^{-1}),$$

where

$$A = E \left[\frac{\lambda^2}{\phi_{H0}} \frac{\partial h_1^H(\theta^g)}{\partial \theta^g} \frac{\partial h_1^H(\theta^g)}{\partial \theta^{g\top}} \Big|_{\theta^g = \theta_0^g} + \frac{(1-\lambda)^2}{\phi_{L0}} \frac{\partial h_1^L(\theta^g)}{\partial \theta^g} \frac{\partial h_1^L(\theta^g)}{\partial \theta^{g\top}} \Big|_{\theta^g = \theta_0^g} \right],$$

$$B = E \left[\frac{\lambda^2 \varphi_1^H(\theta_0)}{\phi_{H0}^2} \frac{\partial h_1^H(\theta^g)}{\partial \theta^g} \frac{\partial h_1^H(\theta^g)}{\partial \theta^{g\top}} \Big|_{\theta^g = \theta_0^g} + \frac{(1-\lambda)^2 \varphi_1^L(\theta_0)}{\phi_{L0}^2} \frac{\partial h_1^L(\theta^g)}{\partial \theta^g} \frac{\partial h_1^L(\theta^g)}{\partial \theta^{g\top}} \Big|_{\theta^g = \theta_0^g} \right].$$

The GARCH parameters are functions of θ . For example, $\omega^g = \lambda\omega_H^g + (1-\lambda)\omega_L^g$, $\alpha^g = \lambda\alpha_H^g + (1-\lambda)\alpha_L^g$, $\beta^g = \lambda\beta_H^g + (1-\lambda)\beta_L^g$, where $\alpha_H^g, \alpha_L^g, \beta_H^g, \beta_L^g$ are defined in Theorem ???. Thus, using the delta method and Slutsky's theorem, we can show that when $\frac{\partial f(\theta^g)}{\partial \theta^g} \Big|_{\theta^g = \theta_0^g} \neq 0$,

$$T_{f,n} = \frac{\sqrt{n}(f(\hat{\theta}^g) - f(\theta_0^g))}{\sqrt{\nabla f(\hat{\theta}^g)^\top (\hat{A}^{-1} \hat{B} \hat{A}^{-1})^{-1} \nabla f(\hat{\theta}^g)}} \xrightarrow{d} N(0, 1), \quad (3.8)$$

where $\nabla f(\hat{\theta}^g) = \frac{\partial f(\theta^g)}{\partial \theta^g} \Big|_{\theta^g = \hat{\theta}^g}$ and \hat{A} and \hat{B} are consistent estimators of A and B , respectively. To evaluate the asymptotic variances of the GARCH parameter estimators, we first need to estimate A and B . We use the following estimators,

$$\hat{A}(\theta^g) = -\frac{\partial^2 \hat{L}_{n,m}(\theta^g)}{\partial \theta^g \partial \theta^{g\top}} \quad \text{and} \quad \hat{B}(\theta^g) = \frac{1}{n} \sum_{i=1}^n \frac{\partial \hat{l}_i(\theta^g)}{\partial \theta^g} \frac{\partial \hat{l}_i(\theta^g)}{\partial \theta^{g\top}},$$

and

$$\hat{l}_i(\theta^g) = \frac{(RV_i - \lambda \hat{h}_i^H(\theta^g))^2}{\hat{\phi}_H} + \frac{\left((X_i - X_{\lambda+i-1})^2 - (1-\lambda) \hat{h}_i^L(\theta^g) \right)^2}{\hat{\phi}_L},$$

and $\hat{h}_i^H(\theta^g)$, $\hat{h}_i^L(\theta^g)$ are defined in (3.1) and (3.2), respectively. Under some stationary condition, we can establish its consistency. Then, using the proposed Z-statistics $T_{f,n}$ in (3.8), we can conduct

the hypothesis tests based on the standard normal distribution.

4 A simulation study

We conducted simulations to check the finite sample performance of the proposed estimation methods. We generated the log-prices for n days with frequency $1/m^{all}$ for each day and let $t_{d,j} = d - 1 + j/m^{all}$, $d = 1, \dots, n, j = 0, \dots, m^{all}$. We chose the closed time λ as $6.5/24$, which corresponds to 6.5 trading hours. The true log-price follows the OGI model in Definition 1. The parameter setup is presented in the supplement document. To generate the jump, we simply set the jump size as $|J_t| = 0.05$ and the signs of the jumps were randomly generated. Λ_t was generated using a Poisson distribution with mean 10 during the open-to-close period. For the open-to-close period, we generated the noisy observations. The detail setup can be found in the supplement document. To generate the true process, we chose $m^{all} = 43,200$, which equals the number of every 2 seconds in a one-day period. We varied n from 100 to 500 and m from 390 to 11,700, which correspond to the numbers of 1 minute and every 2 seconds in the open-to-close period, respectively. We repeated the whole procedure 500 times.

Table 1 reports the mean absolute errors (MAE), $|\hat{\theta} - \theta_0|$ of the WLSE estimates with $n = 100, 200, 500$ and $m = 390, 1170, 11700$ and the true vol. From Table 1, we find that the mean absolute errors usually decrease as the number of high-frequency observations or low-frequency observations increases. The close-to-open period parameters, $\omega_L^g, \alpha_L^g, \beta_L^g$, are mainly dependent on the number of low-frequency observations, whereas the open-to-close period parameters, $\omega_H^g, \gamma, \alpha_H^g, \beta_H^g$, are dependent on the number of both the high-frequency and low-frequency observations. This is because the close-to-open period parameters are estimated based on only the low-frequency data, whereas the open-to-close period parameters, $\omega_H^g, \gamma, \alpha_H^g, \beta_H^g$, are estimated based on both the high-frequency and low-frequency data. This result supports the theoretical findings in Section

Table 1: Mean absolute errors (MAE) for the WLSE estimates with $n = 100, 200, 500$ and $m = 390, 1170, 2340$ and the true vol.

n	m	MAE $\times 10^2$						
		ω_H^g	ω_L^g	γ	α_H^g	α_L^g	β_H^g	β_L^g
100	390	0.0383	0.0497	0.2329	0.1627	0.2145	0.0455	0.1014
	1170	0.0383	0.0498	0.2325	0.1626	0.2141	0.0453	0.1013
	2340	0.0291	0.0484	0.1696	0.1064	0.2307	0.0299	0.1024
	True vol	0.0231	0.0447	0.1483	0.0817	0.2143	0.0233	0.1023
200	390	0.0247	0.0338	0.1619	0.1444	0.1593	0.0380	0.0685
	1170	0.0247	0.0338	0.1615	0.1445	0.1593	0.0378	0.0685
	2340	0.0191	0.0343	0.1091	0.0781	0.1645	0.0229	0.0730
	True vol	0.0136	0.0307	0.0880	0.0513	0.1583	0.0164	0.0749
500	390	0.0159	0.0230	0.1191	0.1329	0.1171	0.0329	0.0446
	1170	0.0159	0.0230	0.1191	0.1330	0.1173	0.0328	0.0446
	2340	0.0134	0.0235	0.0726	0.0586	0.1079	0.0190	0.0490
	True vol	0.0082	0.0212	0.0545	0.0330	0.1053	0.0095	0.0519

3.

To check the asymptotic normality of the GARCH parameters $(\omega^g, \gamma, \alpha^g, \beta^g)$, we calculated the Z-statistics defined in Section 3.3. Figure 1 draws the standard normal quantile-quantile plots of the Z-statistics estimates of ω^g , γ , α^g , and β^g for $n = 500$ and $m = 390, 1170, 11700$ and true volatility. Figure 1 shows that, as the realized volatility closes to the true integrated volatility, the Z-statistics close to the standard normal distribution. This result agrees with the theoretical conclusions in Section 3. Thus, based on the proposed Z-statistics, we can conduct hypothesis tests using the standard normal distribution.

One of our main goals in this paper is to predict future volatility. We therefore examined the out-of-sample performance of estimating the one-day-ahead GARCH volatility $h_{n+1}(\theta_0)$. To estimate future GARCH volatility, we employed the proposed conditional GARCH volatility estimator $\hat{h}_{n+1}(\hat{\theta})$, realized GARCH volatility estimator (Hansen et al., 2012; Song et al., 2020) with only the open-to-close high-frequency observations, discrete GARCH(1,1) volatility estimator with the open-to-open log-returns, and sample variance of the open-to-open log-returns using the in-sample

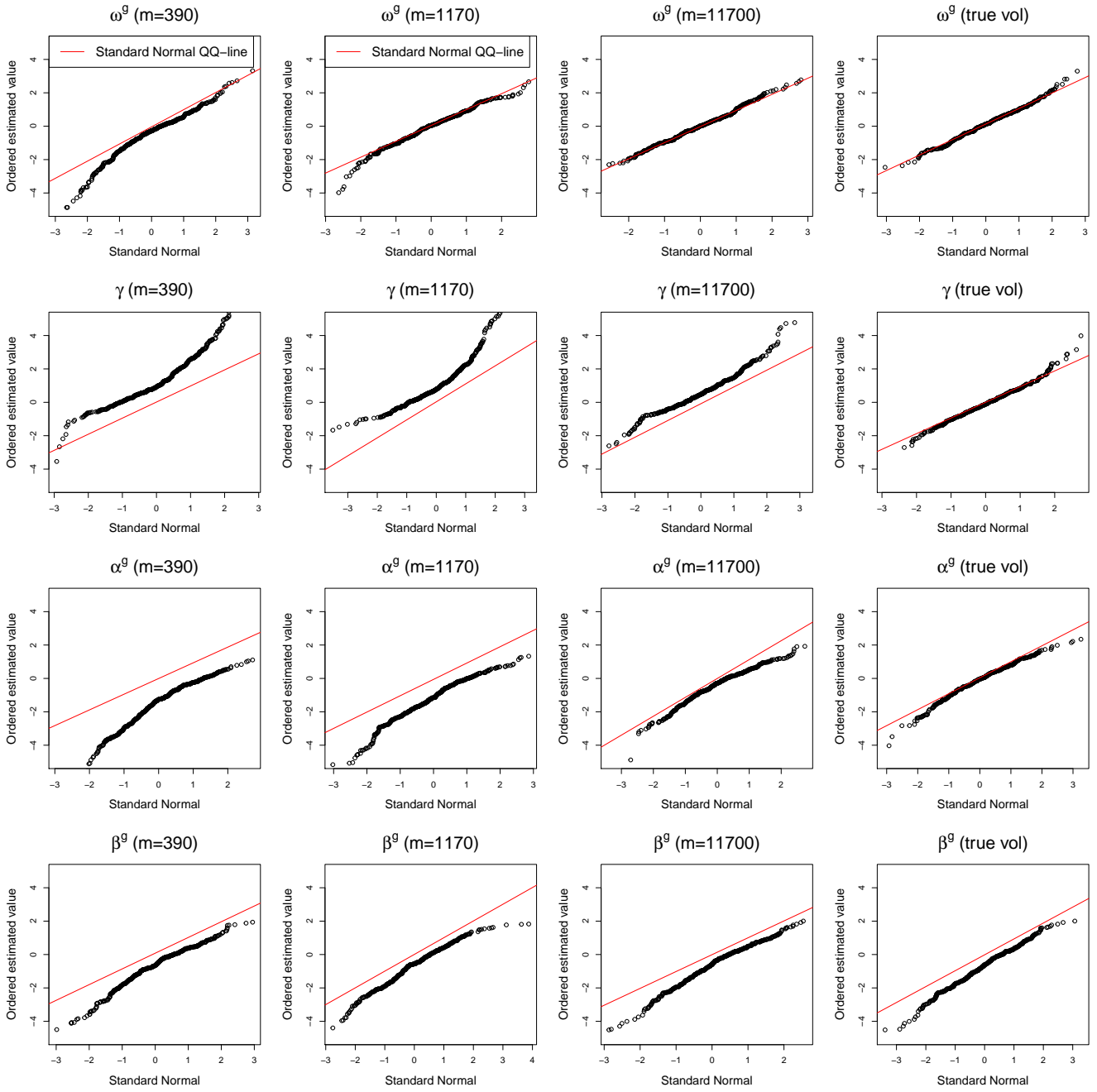


Figure 1: Standard normal quantile-quantile plots of the Z-statistics estimates of ω^g , γ , α^g , and β^g for $n = 500$ and $m = 370, 1170, 11700$ and true volatility. The red real line denotes the best linear fit line, which illustrates perfect standard normal distribution.

data. For example, the realized GARCH volatility has the following GARCH form:

$$h_n(\theta) = \omega + \gamma h_{n-1}(\theta) + \alpha R V_{n-1},$$

and the discrete GARCH(1,1) has the following GARCH form:

$$h_n(\theta) = \omega + \gamma h_{n-1}(\theta) + \beta(X_{n-1} - X_{n-2})^2.$$

We then adopted the QMLE method with the Gaussian quasi-likelihood function to estimate their GARCH parameters. Because the realized GARCH volatility estimator only covers the open-to-close period, we magnified the estimator by multiplying it with $(1 + \text{mean}[OV/RV])$ to match the magnitude, where OV is the overnight return squares and RV is the open-to-close realized volatility. We call this the adjusted realized GARCH volatility. Finally, we also consider other estimation procedures based on Theorem 1 (a). For example, we estimate the open-to-close and close-to-open separately, as described in the first step in Section 3. That is, without the common γ assumption, we make inferences for $h_n^H(\theta)$ and $h_n^L(\theta)$ separately, using the QMLE method with the normal likelihood function. We call this the separate OGI (S-OGI) model. In contrast, we estimate the open-to-open conditional volatility $h_n(\theta)$ directly. Specifically, Theorem 1 (a) shows that the conditional volatility is

$$h_n(\theta^g) = \omega^g + \gamma h_{n-1}(\theta) + \frac{\alpha^g}{1 - \lambda} RV_{n-1} + \frac{\beta^g}{\lambda} (X_{n-1} - X_{\lambda+n-2})^2.$$

Then we estimate the GARCH parameter $(\omega^g, \gamma, \alpha^g, \beta^g)$ using the QMLE method with $RV + OV$ as the proxy. We call this the aggregated OGI (A-OGI) model. We note that this model can be considered as the realized GARCH model with the additional overnight innovation term. We measure the mean absolute errors with the one-day-ahead sample period over 500 samples as follows:

$$\frac{1}{500} \sum_{i=1}^{500} |\widehat{\text{var}}_{n+1,i} - h_{n+1,i}(\theta_0)|,$$

where $\widehat{\text{var}}_{n+1,i}$ is one of the above future volatility estimators at the i th sample path given the

available information at time n .

We report the mean absolute errors for the OGI, S-OGI, A-OGI, realized GARCH, adjusted realized GARCH, GARCH, and sample variance with respect to the OGI against varying the number, n , of the low-frequency observations and the number, m , of the high-frequency observations in Table 2. In Table 2, we find that the OGI models can estimate the one-day-ahead GARCH volatility $h_{n+1}(\theta_0)$ well, but the other estimators cannot account for it well. This may be because, under the OGI model, the market dynamics are explained by the open-to-close high-frequency volatility and squared close-to-open log-returns; however, the other models ignore one of the factors. Compared to estimation methods for the OGI models, the WLSE yields better performance than the others. One possible explanation for this is that the WLSE procedure gives more weight to the high-frequency observations, and this helps reduce the estimation errors. From these results, we can conjecture that modeling appropriate overnight processes helps to not only account for market dynamics but also improve the estimation accuracy.

Table 2: Mean absolute errors (MAE) for the OGI, S-OGI, A-OGI, realized GARCH, adjusted realized GARCH, GARCH, and sample variance with respect to the OGI with $n = 100, 200, 500$, and $m = 390, 1170, 11700$, and true volatility.

n	m	MAE $\times 10$						
		OGI	S-OGI	A-OGI	Adj-Realized	Realized	GARCH	Sample
100	390	0.3828	0.4877	0.4346	0.8357	1.4920	0.7644	1.5040
	1170	0.3612	0.4500	0.4224	0.4574	1.4287	0.7644	1.4415
	2340	0.3328	0.4196	0.4038	0.3531	1.3775	0.7644	1.3968
	True vol	0.2991	0.4165	0.3712	0.2966	1.4079	0.7644	1.4320
200	390	0.3090	0.3561	0.3356	0.8186	1.4986	0.5170	1.5027
	1170	0.2847	0.3385	0.3228	0.4567	1.4325	0.5170	1.4386
	2340	0.2570	0.3033	0.2909	0.3365	1.3821	0.5170	1.3873
	True vol	0.2353	0.2881	0.2674	0.2855	1.4086	0.5170	1.4163
500	390	0.2460	0.2527	0.2542	0.7983	1.5168	0.4298	1.5295
	1170	0.2083	0.2271	0.2280	0.4270	1.4526	0.4298	1.4566
	2340	0.1762	0.1984	0.2004	0.3270	1.4013	0.4298	1.4029
	True vol	0.1462	0.1735	0.1744	0.2840	1.4271	0.4298	1.4316

5 An empirical study

We applied the proposed OGI model to real trading high-frequency data. We obtained the top 5 trading volume assets (BAC, FCX, INTC, MSFT, MU) intra-day data from January 2010 to December 2016 from the TAQ database in the Wharton Research Data Services (WRDS) system, 1762 trading days in total. We defined the trading hours from 9:30 to 16:00 as the open-to-close period and the overnight period from 16:00 to the following-day 9:30 as the close-to-open period, that is, $\lambda = 6.5/24$. We used the log-prices and adopted the jump robust PRV estimation procedure in (??) in the supplement document to estimate open-to-close integrated volatility. In the empirical study, we chose the tuning parameter c_τ as 10 times the sample standard deviation of pre-averaged prices $m^{1/8}\bar{Y}(t_{d,k})$. We fixed the in-sample period as 500 days and used the rolling window scheme to estimate the parameters.

To check the relative importance of each OGI model component, we report the average proportion of jumps, and the mean and standard deviation of the PRV, squared overnight return, and estimated GARCH volatility from the OGI model in Table 3. From Table 3, we find that the magnitude of squared overnight returns is comparable to that of PRV, and the squared overnight returns have a greater standard deviation. This result leads us to conjecture that the overnight risk usually significantly affects the volatility dynamics structure.

Table 3: Average of the jump proportion, and mean and standard deviations for pre-averaging realized volatility (PRV), overnight volatility (OV), and conditional GARCH.

Stock	Jump	Mean $\times 10^4$			SD $\times 10^4$		
		PRV	OV	GARCH	PRV	OV	GARCH
BAC	0.148	1.719	1.139	3.204	1.577	3.195	2.571
FCX	0.167	5.423	3.399	9.080	8.721	12.438	11.561
INTC	0.158	1.090	0.750	1.906	0.969	3.675	1.201
MSFT	0.141	0.996	0.953	1.893	1.037	5.254	1.088
MU	0.171	4.104	2.336	6.529	2.990	11.141	2.732

For a comparison, we calculated the OGI, S-OGI, A-OGI, discrete GARCH(1,1), and adjusted

realized GARCH volatilities defined in Section 4 and the GJR GARCH (1,1) (Glosten et al., 1993). To check the performance of the ARFI-type model, we adopted the HAR-RV model (Corsi, 2009) and log-HAR-RV model with the bias correction (Demetrescu et al., 2020). For the log-HAR-RV model, we apply the HAR model on the logarithm of the realized volatility and multiply $\exp(\hat{\sigma}^2/2)$ to the forecast value, where $\hat{\sigma}^2$ is the consistent estimator of the error variance for the HAR model on the log-realized volatility. Then, we magnified these two estimators by multiplying $(1 + \text{mean}[OV/RV])$ to match the scale of the whole day variation, which are called “adjusted HAR” and “adjusted log-HAR,” respectively. To check the leverage effect, we also considered some variations of the OGI model as follows:

$$h_n(\theta) = \left(\omega^g + \gamma h_{n-1}(\theta) + \frac{\alpha^g + I_{n-1}^H a}{\lambda} \int_{n-2}^{n-2+\lambda} \sigma_t^2(\theta) dt + \frac{\beta^g + I_{n-1}^L b}{1 - \lambda} (X_{n-1} - X_{n-2+\lambda})^2 \right),$$

where $I_n^H = \mathbf{1}_{\{X_{n-1+\lambda} - X_{n-1} < c_H\}}$, $I_n^L = \mathbf{1}_{\{X_n - X_{n-1+\lambda} < c_L\}}$, a , b , c_H and c_L are additional parameters.

To estimate the parameters, we adopted the QMLE method, which is referred to as GJR-OGI.

To measure the performance of the volatility, we used the mean squared prediction errors (MSPE) and QLIKE (Patton, 2011) as follows:

$$MSPE = \frac{1}{n} \sum_{i=1}^n (Vol_i - (RV_i + (X_i - X_{\lambda+i-1})^2))^2,$$

$$QLIKE = \frac{1}{n} \sum_{i=1}^n \log Vol_i + \frac{RV_i + (X_i - X_{\lambda+i-1})^2}{Vol_i},$$

where Vol_i is one of the OGI, S-OGI, A-OGI, GJR-OGI, GJR GARCH, discrete GARCH, adjusted realized GARCH, adjusted HAR, and adjusted log-HAR volatilities, and we used $RV_i + (X_i - X_{\lambda+i-1})^2$ as the nonparametric daily volatility estimator. We predicted the one-day-ahead conditional expected volatility using the in-sample period data. Also, to check the significance of the difference in performances, we conducted the Diebold and Mariano (DM) test (Diebold and

Mariano, 1995) for the MSPE and QLIKE. We compared the OGI with other models. Table 4 reports the average rank and the number of the first rank of MSPEs and QLIKES for the nine models over the five assets. Table 5 reports the full MSPEs and QLIKES results, and Table 6 shows the p-values for the DM tests. From Tables 4 and 5, we find that incorporating the squared overnight returns as a new innovation helps explain the market dynamics. From Tables 4–6, we find that the OGI model shows the best performance overall. This may be because the weighted least squared estimation method helps improve the volatility prediction accuracy.

Table 4: Average rank of MSPEs and QLIKES for the OGI, S-OGI, A-OGI, GJR-OGI, GJR, discrete GARCH, adjusted realized GARCH, adjusted HAR, and adjusted log-HAR. In the parenthesis, we report the number of the first rank among competitors.

	OGI	S-OGI	A-OGI	GJR-OGI	GJR	GARCH	Adj-Realized	Adj-HAR	Adj-log-HAR
MSPE	2.2 (3)	2.8 (1)	4.0 (0)	6.2 (0)	9.0 (0)	7.2 (0)	5.0 (0)	5.2 (0)	3.4 (1)
QLIKE	1.6 (4)	3.6 (0)	3.8 (1)	3.4 (0)	8.4 (0)	8.6 (0)	6.0 (0)	4.6 (0)	5.0 (0)

Table 5: MSPEs and QLIKES for the OGI, S-OGI, A-OGI, GJR-OGI, GJR, discrete GARCH, adjusted realized GARCH, adjusted HAR, and adjusted log-HAR.

Stock		OGI	S-OGI	A-OGI	GJR-OGI	GJR	GARCH	Adj-Realized	Adj-HAR	Adj-log-HAR
BAC	MSPE $\times 10^7$	1.194	1.118	1.132	1.153	2.110	1.945	1.267	1.262	1.257
	QLIKE	-7.354	-7.375	-7.376	-7.366	-7.205	-7.260	-7.336	-7.334	-7.340
FCX	MSPE $\times 10^6$	1.753	1.894	1.898	2.024	5.883	4.212	2.362	2.377	2.275
	QLIKE	-6.449	-6.384	-6.400	-6.387	-6.254	-6.311	-6.352	-6.359	-6.367
INTC	MSPE $\times 10^7$	1.499	1.504	1.540	1.586	1.592	1.548	1.492	1.495	1.464
	QLIKE	-7.676	-7.672	-7.666	-7.676	-7.644	-7.642	-7.671	-7.669	-7.668
MSFT	MSPE $\times 10^7$	2.905	2.932	2.992	3.099	3.143	2.971	2.945	2.957	2.907
	QLIKE	-7.596	-7.588	-7.576	-7.590	-7.573	-7.547	-7.585	-7.595	-7.591
MU	MSPE $\times 10^6$	1.328	1.354	1.332	1.471	1.487	1.438	1.371	1.358	1.356
	QLIKE	-6.375	-6.364	-6.367	-6.362	-6.312	-6.063	-6.358	-6.365	-6.360

To check the benefit of using the overnight information, we employed a utility based framework (?Demetrescu et al., 2020; ?). Specifically, we assume that there is a risk-averse person who invests part of his wealth $x_i \in [0, 1]$ in specified asset and holds the remaining part $1 - x_i$ at time $i - 1$. The mean-variance utility function is defined as

$$EU(R_i) = E[x_i R_i | \mathcal{F}_{i-1}] - \frac{\xi}{2} \text{Var}[x_i R_i | \mathcal{F}_{i-1}],$$

Table 6: The p-values for the test statistic DM based on the MSPE and QLIKE for the S-OGI, A-OGI, GJR-OGI, GJR, discrete GARCH, adjusted realized GARCH, adjusted HAR, and adjusted log-HAR with respect to the OGI.

Stock		S-OGI	A-OGI	GJR-OGI	GJR	GARCH	Adj-Realized	Adj-HAR	Adj-log-HAR
BAC	MSPE	0.999	0.823	0.730	0.000	0.000	0.245	0.265	0.283
	QLIKE	0.999	0.999	0.975	0.000	0.000	0.072	0.050	0.148
FCX	MSPE	0.011	0.035	0.059	0.000	0.000	0.000	0.000	0.000
	QLIKE	0.000	0.001	0.021	0.000	0.000	0.000	0.002	0.004
INTC	MSPE	0.328	0.019	0.145	0.054	0.159	0.563	0.542	0.817
	QLIKE	0.371	0.280	0.479	0.010	0.013	0.379	0.238	0.311
MSFT	MSPE	0.015	0.001	0.020	0.004	0.060	0.112	0.170	0.463
	QLIKE	0.164	0.036	0.343	0.158	0.000	0.276	0.469	0.395
MU	MSPE	0.110	0.105	0.069	0.000	0.000	0.000	0.004	0.003
	QLIKE	0.191	0.185	0.063	0.036	0.122	0.029	0.091	0.100

where $\xi > 0$ is the risk aversion coefficient and R_i is the daily log-return. Then, the optimal allocation has the following form:

$$x_i = \frac{1}{\xi} \frac{E[R_i | \mathcal{F}_{i-1}]}{\text{Var}[R_i | \mathcal{F}_{i-1}]},$$

where $E[R_i | \mathcal{F}_{i-1}]$ and $\text{Var}[R_i | \mathcal{F}_{i-1}]$ are replaced by their forecasts. Since it is difficult to predict the expectation $E[R_i | \mathcal{F}_{i-1}]$ in practice, we replace it with the previous day's log-return based on the martingale assumption on the daily return process. Also, the variance $\text{Var}[R_i | \mathcal{F}_{i-1}]$ is replaced by one of the OGI, S-OGI, A-OGI, GJR-OGI, GJR, discrete GARCH, realized GARCH, HAR, and log-HAR volatilities. For the OGI, S-OGI, A-OGI, GJR-OGI, GJR, and GARCH, we used the open-to-open returns for R_i , while the open-to-close returns were used for the realized GARCH, HAR, and log-HAR. Then, we obtained \hat{x}_i and set $x_i^* = \hat{x}_i \mathbf{1}_{\{\hat{x}_i \in [0,1]\}} + \mathbf{1}_{\{\hat{x}_i > 1\}}$ to make the investment feasible and prevent the short-sellings. Finally, the resulting returns $R_i^* = x_i^* R_i$ were used to measure the economic performances. Specifically, with the mean \bar{R}^* and standard deviation \bar{S}^* of the returns R_i^* , we calculated the Sharpe ratio $SR^* = \bar{R}^* / \bar{S}^*$ and expected utility $EU^* = \bar{R}^* - \frac{\xi}{2} (\bar{S}^*)^2$. Table 7 reports the Sharpe ratios and expected utilities for the nine models for $\xi = 2.5, 5$ over the five assets. As seen in Table 7, the models with the open-to-open information show better performance than other models. This may indicate that considering overnight period helps obtain the additional

economic gains. When comparing the models with the open-to-open information, the OGI-based models do not significantly outperform the GJR and GARCH models. This may be because the future return estimator often has the huge errors in practice. From this result, we can conjecture that the overnight period is significant in terms of investing strategy.

Table 7: Sharpe ratios (SR^*) and expected utilities (EU^*) for the OGI, S-OGI, A-OGI, GJR-OGI, GJR, discrete GARCH, realized GARCH, HAR, and log-HAR for $\xi = 2.5, 5$ and five assets.

Risk aversion	Stock		OGI	S-OGI	A-OGI	GJR-OGI	GJR	GARCH	Realized	HAR	Log-HAR
$\xi=2.5$	BAC	$SR^* \times 10^2$	3.974	3.952	3.944	3.911	3.936	3.882	-5.173	-5.167	-5.166
		$EU^* \times 10^4$	3.116	3.086	3.073	3.027	3.062	2.985	-6.864	-6.854	-6.855
	FCX	$SR^* \times 10^2$	-2.891	-2.993	-3.004	-3.002	-2.894	-2.869	-5.008	-5.002	-4.996
		$EU^* \times 10^3$	-1.333	-1.350	-1.352	-1.357	-1.318	-1.312	-1.386	-1.386	-1.386
	INTC	$SR^* \times 10^2$	2.302	2.301	2.305	2.307	2.323	2.306	5.368	5.370	5.363
		$EU^* \times 10^4$	1.060	1.059	1.063	1.064	1.079	1.064	3.441	3.443	3.437
	MSFT	$SR^* \times 10^2$	2.857	2.909	2.925	2.907	2.848	2.812	2.789	2.769	2.787
		$EU^* \times 10^4$	1.588	1.639	1.654	1.637	1.579	1.543	1.375	1.360	1.374
	MU	$SR^* \times 10^2$	5.875	5.932	5.878	5.839	5.642	5.651	0.007	-0.029	-0.038
		$EU^* \times 10^4$	6.691	6.803	6.695	6.615	6.230	6.250	-2.875	-2.944	-2.955
$\xi=5$	BAC	$SR^* \times 10^2$	3.726	3.813	3.822	3.724	3.703	3.646	-5.018	-5.029	-5.027
		$EU^* \times 10^4$	0.344	0.455	0.466	0.336	0.348	0.252	-8.023	-8.025	-8.032
	FCX	$SR^* \times 10^2$	-2.937	-2.921	-2.998	-2.792	-2.891	-2.842	-5.108	-5.182	-5.182
		$EU^* \times 10^3$	-1.972	-1.940	-1.956	-1.924	-1.898	-1.893	-1.798	-1.818	-1.817
	INTC	$SR^* \times 10^2$	2.483	2.424	2.436	2.466	2.492	2.431	5.199	5.121	5.167
		$EU^* \times 10^4$	0.177	0.120	0.131	0.161	0.183	0.127	2.535	2.473	2.510
	MSFT	$SR^* \times 10^2$	2.550	2.680	2.733	2.665	2.477	2.426	2.492	2.502	2.498
		$EU^* \times 10^4$	0.194	0.317	0.366	0.297	0.134	0.089	0.490	0.497	0.494
	MU	$SR^* \times 10^2$	5.372	5.351	5.314	5.274	5.372	5.162	0.172	0.178	0.169
		$EU^* \times 10^4$	1.264	1.219	1.143	1.093	1.283	0.918	-5.260	-5.259	-5.277

To check the volatility persistence of the nonparametric volatility, we study regression residuals between the nonparametric volatility and estimated conditional volatilities. Specifically, we fitted the following linear model

$$RV_i + (X_i - X_{\lambda+i-1})^2 = a + b \times Vol_i + e_i,$$

where Vol_i is one of the predicted volatilities OGI, S-OGI, A-OGI, GJR-OGI, GJR, discrete GARCH, adjusted realized GARCH, adjusted HAR, and adjusted log-HAR. Then, we calculated the regression residuals, \hat{e}_i , for each model and checked their auto-correlations over lag

$L = 1, \dots, 30$. Table 8 reports the average rank and the number of the first rank for the first and max absolute auto-correlations from the nine models. In the supplement document, we draw the auto-correlation function (ACF) of the regression residuals for each model and asset (see Figure ??). From Table 8 and Figure ??, we find that the OGI, S-OGI, A-OGI, and GJR-OGI models show better performance than other estimators overall. That is, the OGI-based models can explain the market dynamics in the volatility time series.

Table 8: Average ranks in order from the smallest to the biggest for the first and max absolute auto-correlations over lag $L = 1, \dots, 30$ for the OGI, S-OGI, A-OGI, GJR-OGI, GJR, discrete GARCH, adjusted realized GARCH, adjusted HAR, and adjusted log-HAR. In the parenthesis, we report the number of the first rank among competitors.

	OGI	S-OGI	A-OGI	GJR-OGI	GJR	GARCH	Adj-Realized	Adj-HAR	Adj-log-HAR
First	1.8 (3)	3.8 (0)	4.0 (0)	3.0 (1)	4.6 (1)	6.4 (0)	6.8 (0)	6.6 (0)	8.0 (0)
Max	2.8 (1)	3.0 (2)	3.8 (0)	5.6 (0)	6.8 (0)	6.4 (0)	5.4 (0)	4.8 (1)	6.4 (1)

We examined the performance of the proposed method in measuring one-day-ahead VaR. To evaluate VaR, we first predicted the one-day-ahead conditional expected volatility by the OGI, S-OGI, A-OGI, GJR-OGI, GJR, discrete GARCH, adjusted realized GARCH, adjusted HAR, and adjusted log-HAR using the in-sample period data. We then calculated the quantiles by historical standardized daily returns. Specifically, we standardized the in-sample daily returns by the fitted conditional volatilities. Then, we calculated the sample quantiles for 0.01, 0.02, 0.05, 0.1, 0.2 and with the sample quantile estimates and predicted volatility, we obtained the one-day ahead VaR values. We fixed the in-sample period as 500 days and used the rolling window scheme.

To backtest the estimated VaR, we conducted the likelihood ratio unconditional coverage (LRuc) test (Kupiec, 1995), the likelihood ratio conditional coverage (LRcc) Christoffersen (1998), and the dynamic quantile (DQ) test with lag 4 (Engle and Manganelli, 2004). Table 9 reports the number of cases where p-value is bigger than 0.05 for the five assets and $q_0 = 0.01, 0.02, 0.05, 0.1, 0.2$ based on the LRuc, LRcc and DQ tests. In the supplement document, we draw the scatterplots for the p-values of LRuc, LRcc, and DQ tests for the nine models with $q_0 = 0.01, 0.02, 0.05, 0.1, 0.2$ (see

Figure ??). As seen in Table 9 and Figure ??, the OGI model shows the best performance for all hypothesis tests. This result shows that the overnight risk is important to account for whole-day market dynamics, and the OGI process can account for market dynamics by utilizing the overnight risk information. In contrast, other OGI-based models show relatively worse performance. This finding prompts us to speculate that it may help improve estimation accuracy by estimating the open-to-close and close-to-open separately with the weighted least squared estimation method under the common γ condition.

Table 9: Number of cases where p-value is bigger than 0.05 for the OGI, S-OGI, A-OGI, GJR-OGI, GJR, discrete GARCH, adjusted realized GARCH, adjusted HAR, and adjusted log-HAR for the 5 assets and $q_0 = 0.01, 0.02, 0.05, 0.1, 0.2$ based on the LRuc, LRcc and DQ tests.

	OGI	S-OGI	A-OGI	GJR-OGI	GJR	GARCH	Adj-Realized	Adj-HAR	Adj-log-HAR
LRuc	25	17	20	18	22	21	21	21	18
LRcc	25	22	20	19	20	21	21	21	16
DQ	18	7	6	10	18	10	6	11	0

6 Conclusion

In this paper, we introduce the diffusion process, which can explain the whole-day volatility dynamics. Specifically, the proposed OGI model can account for the different dynamic structures for the open-to-close and close-to-open periods. To do this, we introduced the weighted QMLE procedure and showed its asymptotic properties. In the empirical study, we found the benefit of incorporating the overnight information. The models with overnight innovation term perform better than other models for the prediction of daily volatility, utility based analysis, and volatility persistence analysis. It suggests that incorporating the overnight information helps account for the dynamic structure of the daily total variation. On the other hand, the OGI model outperforms other OGI-based models in terms of the prediction of daily volatility, analysis of volatility persistence, and one-day-ahead VaR measurement. It reveals that the weighted least squared estimation method with the common γ condition helps obtain better estimation accuracy.

In practice, we often observe zero returns (Francq and Sucarrat, 2021). However, the proposed diffusion process cannot account for the zero return phenomena. Thus, it is an interesting future study to develop a diffusion process, which can account for the zero returns, and to investigate its effect.

References

- Admati, A. R. and Pfleiderer, P. (1988). A theory of intraday patterns: Volume and price variability. *The Review of Financial Studies*, 1(1):3–40.
- Aït-Sahalia, Y., Fan, J., and Xiu, D. (2010). High-frequency covariance estimates with noisy and asynchronous financial data. *Journal of the American Statistical Association*, 105(492):1504–1517.
- Aït-Sahalia, Y., Jacod, J., and Li, J. (2012). Testing for jumps in noisy high frequency data. *Journal of Econometrics*, 168(2):207–222.
- Aït-Sahalia, Y. and Xiu, D. (2016). Increased correlation among asset classes: Are volatility or jumps to blame, or both? *Journal of Econometrics*, 194(2):205–219.
- Andersen, T. G., Bollerslev, T., Diebold, F. X., and Labys, P. (2003). Modeling and forecasting realized volatility. *Econometrica*, 71(2):579–625.
- Andersen, T. G., Bollerslev, T., and Huang, X. (2011). A reduced form framework for modeling volatility of speculative prices based on realized variation measures. *Journal of Econometrics*, 160(1):176–189.
- Andersen, T. G., Thyrgaard, M., and Todorov, V. (2019). Time-varying periodicity in intraday volatility. *Journal of the American Statistical Association*, 114(528):1695–1707.

- Barndorff-Nielsen, O. E., Hansen, P. R., Lunde, A., and Shephard, N. (2008). Designing realized kernels to measure the ex post variation of equity prices in the presence of noise. *Econometrica*, 76(6):1481–1536.
- Barndorff-Nielsen, O. E. and Shephard, N. (2006). Econometrics of testing for jumps in financial economics using bipower variation. *Journal of financial Econometrics*, 4(1):1–30.
- Bollerslev, T. (1986). Generalized autoregressive conditional heteroskedasticity. *Journal of econometrics*, 31(3):307–327.
- Christoffersen, P. F. (1998). Evaluating interval forecasts. *International economic review*, pages 841–862.
- Corsi, F. (2009). A simple approximate long-memory model of realized volatility. *Journal of Financial Econometrics*, 7(2):174–196.
- Corsi, F., Pirino, D., and Reno, R. (2010). Threshold bipower variation and the impact of jumps on volatility forecasting. *Journal of Econometrics*, 159(2):276–288.
- Demetrescu, M., Golosnoy, V., and Titova, A. (2020). Bias corrections for exponentially transformed forecasts: Are they worth the effort? *International Journal of Forecasting*, 36(3):761–780.
- Diebold, F. X. and Mariano, R. S. (1995). Comparing predictive accuracy. *Journal of Business and Economic Statistics*, 13(3):253–263.
- Duffie, D. and Pan, J. (1997). An overview of value at risk. *Journal of derivatives*, 4(3):7–49.
- Engle, R. F. (1982). Autoregressive conditional heteroscedasticity with estimates of the variance of united kingdom inflation. *Econometrica: Journal of the Econometric Society*, pages 987–1007.
- Engle, R. F. and Manganelli, S. (2004). Caviar: Conditional autoregressive value at risk by regression quantiles. *Journal of Business & Economic Statistics*, 22(4):367–381.

- Fan, J. and Kim, D. (2018). Robust high-dimensional volatility matrix estimation for high-frequency factor model. *Journal of the American Statistical Association*, 113(523):1268–1283.
- Fan, J. and Wang, Y. (2007). Multi-scale jump and volatility analysis for high-frequency financial data. *Journal of the American Statistical Association*, 102(480):1349–1362.
- Francq, C. and Sucarrat, G. (2021). Volatility estimation when the zero-process is nonstationary. *Journal of Business & Economic Statistics*, pages 1–14.
- Glosten, L. R., Jagannathan, R., and Runkle, D. E. (1993). On the relation between the expected value and the volatility of the nominal excess return on stocks. *Journal of Finance*, 48(5):1779–1801.
- Hansen, P. R., Huang, Z., and Shek, H. H. (2012). Realized garch: a joint model for returns and realized measures of volatility. *Journal of Applied Econometrics*, 27(6):877–906.
- Hansen, P. R. and Lunde, A. (2005). A realized variance for the whole day based on intermittent high-frequency data. *Journal of Financial Econometrics*, 3(4):525–554.
- Hong, H. and Wang, J. (2000). Trading and returns under periodic market closures. *The Journal of Finance*, 55(1):297–354.
- Jacod, J., Li, Y., Mykland, P. A., Podolskij, M., and Vetter, M. (2009). Microstructure noise in the continuous case: the pre-averaging approach. *Stochastic processes and their applications*, 119(7):2249–2276.
- Kim, D. and Fan, J. (2019). Factor garch-itô models for high-frequency data with application to large volatility matrix prediction. *Journal of Econometrics*, 208(2):395–417.
- Kim, D., Liu, Y., and Wang, Y. (2018). Large volatility matrix estimation with factor-based diffusion model for high-frequency financial data. *Bernoulli*, 24(4B):3657–3682.

- Kim, D. and Wang, Y. (2016). Unified discrete-time and continuous-time models and statistical inferences for merged low-frequency and high-frequency financial data. *Journal of Econometrics*, 194:220–230.
- Kim, D., Wang, Y., and Zou, J. (2016). Asymptotic theory for large volatility matrix estimation based on high-frequency financial data. *Stochastic Processes and their Applications*, 126:3527–3577.
- Kupiec, P. H. (1995). Techniques for verifying the accuracy of risk measurement models. *The Journal of Derivatives*, 3(2):73–84.
- Mancini, C. (2004). Estimation of the characteristics of the jumps of a general poisson-diffusion model. *Scandinavian Actuarial Journal*, 2004(1):42–52.
- Markowitz, H. (1952). Portfolio selection. *The journal of finance*, 7(1):77–91.
- Martens, M. (2002). Measuring and forecasting s&p 500 index-futures volatility using high-frequency data. *Journal of Futures Markets: Futures, Options, and Other Derivative Products*, 22(6):497–518.
- Patton, A. J. (2011). Volatility forecast comparison using imperfect volatility proxies. *Journal of Econometrics*, 160(1):246–256.
- Rockafellar, R. T. and Uryasev, S. (2000). Optimization of conditional value-at-risk. *Journal of risk*, 2:21–42.
- Sharpe, W. F. (1964). Capital asset prices: A theory of market equilibrium under conditions of risk. *The journal of finance*, 19(3):425–442.
- Shephard, N. and Sheppard, K. (2010). Realising the future: forecasting with high-frequency-based volatility (heavy) models. *Journal of Applied Econometrics*, 25(2):197–231.

- Song, X., Kim, D., Yuan, H., Cui, X., Lu, Z., Zhou, Y., and Yazhen, W. (2020). Volatility analysis with realized garch-ito models. *Journal of Econometrics*, DOI:10.1016/j.jeconom.2020.07.007.
- Tao, M., Wang, Y., and Chen, X. (2013). Fast convergence rates in estimating large volatility matrices using high-frequency financial data. *Econometric Theory*, 29(04):838–856.
- Taylor, N. (2007). A note on the importance of overnight information in risk management models. *Journal of Banking & Finance*, 31(1):161–180.
- Todorova, N. and Souček, M. (2014). Overnight information flow and realized volatility forecasting. *Finance Research Letters*, 11(4):420–428.
- Tseng, T.-C., Lai, H.-C., and Lin, C.-F. (2012). The impact of overnight returns on realized volatility. *Applied Financial Economics*, 22(5):357–364.
- Xiu, D. (2010). Quasi-maximum likelihood estimation of volatility with high frequency data. *Journal of Econometrics*, 159(1):235–250.
- Zhang, L. (2006). Efficient estimation of stochastic volatility using noisy observations: A multi-scale approach. *Bernoulli*, 12(6):1019–1043.
- Zhang, L., Mykland, P. A., and Aït-Sahalia, Y. (2005). A tale of two time scales: Determining integrated volatility with noisy high-frequency data. *Journal of the American Statistical Association*, 100(472):1394–1411.
- Zhang, X., Kim, D., and Wang, Y. (2016). Jump variation estimation with noisy high frequency financial data via wavelets. *Econometrics*, 4(3):34.

Supplement to “Overnight GARCH-Itô Volatility Models”

June 20, 2022

A Simulation setup

We chose the drift $\mu_t = 0$, and $(\omega_{H1,0}, \omega_{H2,0}, \omega_{L,0}, \gamma_{H,0}, \gamma_{L,0}, \alpha_{H,0}, \alpha_{L,0}, \beta_{H,0}, \beta_{L,0}, \nu_{H,0}, \nu_{L,0}) = (0.02, 0.01, 0.01, 0.6, 0.6, 0.4, 0.1, 0.2, 0.1, 0.4, 0.2)$. In this case, the target GARCH parameter is $(\omega_{H,0}^g, \omega_{L,0}^g, \gamma_0, \alpha_{H,0}^g, \alpha_{L,0}^g, \beta_{H,0}^g, \beta_{L,0}^g) = (0.067, 0.063, 0.36, 0.21, 0.202, 0.128, 0.096)$. For the open-to-close period, we generated the noisy observations as follows:

$$Y_{t_{d,j}} = X_{t_{d,j}} + \epsilon_{t_{d,j}}, \quad \text{for } d = 1, \dots, n, j = 1, \dots, m - 1,$$

where m is the number of high-frequency observations for the open-to-close period, and $\epsilon_{t_{d,j}}$'s are generated from i.i.d. normal distributions with mean zero and standard deviation $0.01 \sqrt{\int_{t_{d-1}}^d \sigma_t^2(\theta) dt}$. To generate the true process, we chose $m^{all} = 43,200$, which equals the number of every 2 seconds in a one-day period. We varied n from 100 to 500 and m from 390 to 11,700, which correspond to the numbers of 1 minute and every 2 seconds in the open-to-close period, respectively. We treated $Y_{t_{d,j}}, j = 1, \dots, m - 1$ as the high-frequency observations and the open and close prices $X_{t_{d,0}}$ and $X_{t_{d,m}}$ as the observed log-prices. To estimate the integrated volatility for the open-to-close period, we employed the jump adjusted pre-averaging realized volatility estimator (Aït-Sahalia and Xiu,

2016; Jacod et al., 2009) as follows:

$$RV_d = \frac{1}{\psi K} \sum_{k=1}^{m-K+1} \left\{ \bar{Y}^2(t_{d,k}) - \frac{1}{2} \hat{Y}^2(t_{d,k}) \right\} \mathbf{1}_{\{|\bar{Y}(t_{d,k})| \leq \tau_m\}}, \quad (\text{A.1})$$

where

$$\begin{aligned} \bar{Y}(t_{d,k}) &= \sum_{l=1}^{K-1} g\left(\frac{l}{K}\right) (Y_{t_{d,k+l}} - Y_{t_{d,k+l-1}}), \quad \psi = \int_0^1 g(t)^2 dt, \\ \hat{Y}^2(t_{d,k}) &= \sum_{l=1}^K \left\{ g\left(\frac{l}{K}\right) - g\left(\frac{l-1}{K}\right) \right\}^2 (Y_{t_{d,k+l-1}} - Y_{t_{d,k+l-2}})^2, \end{aligned}$$

we take the weight function $g(x) = x \wedge (1-x)$ and the bandwidth size $K = \lfloor m^{1/2} \rfloor$, $\mathbf{1}_{\{\cdot\}}$ is an indicator function, and $\tau_m = c_\tau m^{-0.235}$ is a truncation level for the constant c_τ . We chose c_τ as three times the sample standard deviation of the pre-averaged prices $m^{1/8} \bar{Y}(t_{d,k})$.

B Miscellaneous materials

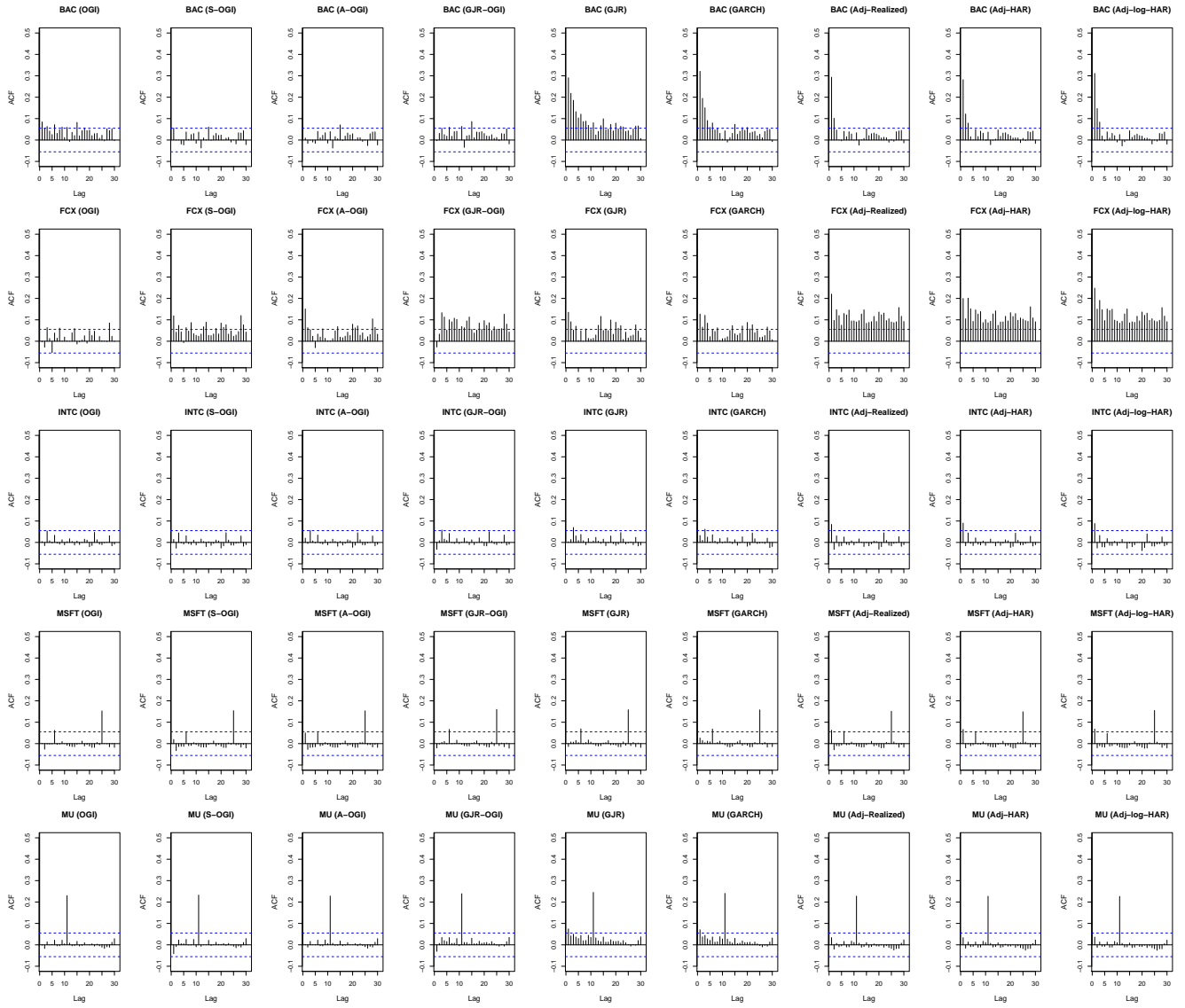


Figure B.1: ACF plots for the regression residuals between the nonparametric volatility and estimated volatility, such as the OGI, S-OGI, A-OGI, GJR-OGI, GJR, discrete GARCH, adjusted realized GARCH, adjusted HAR, and adjusted log-HAR.

C Proofs

C.1 Proof of Theorem ??

Let $P_t = \int_0^t \sigma_t(\theta) dB_t$. Theorem ?? is an immediate consequence of Theorem C1 (a) below.

Theorem C1. *For the OGI model, the integrated volatilities have the following structure.*

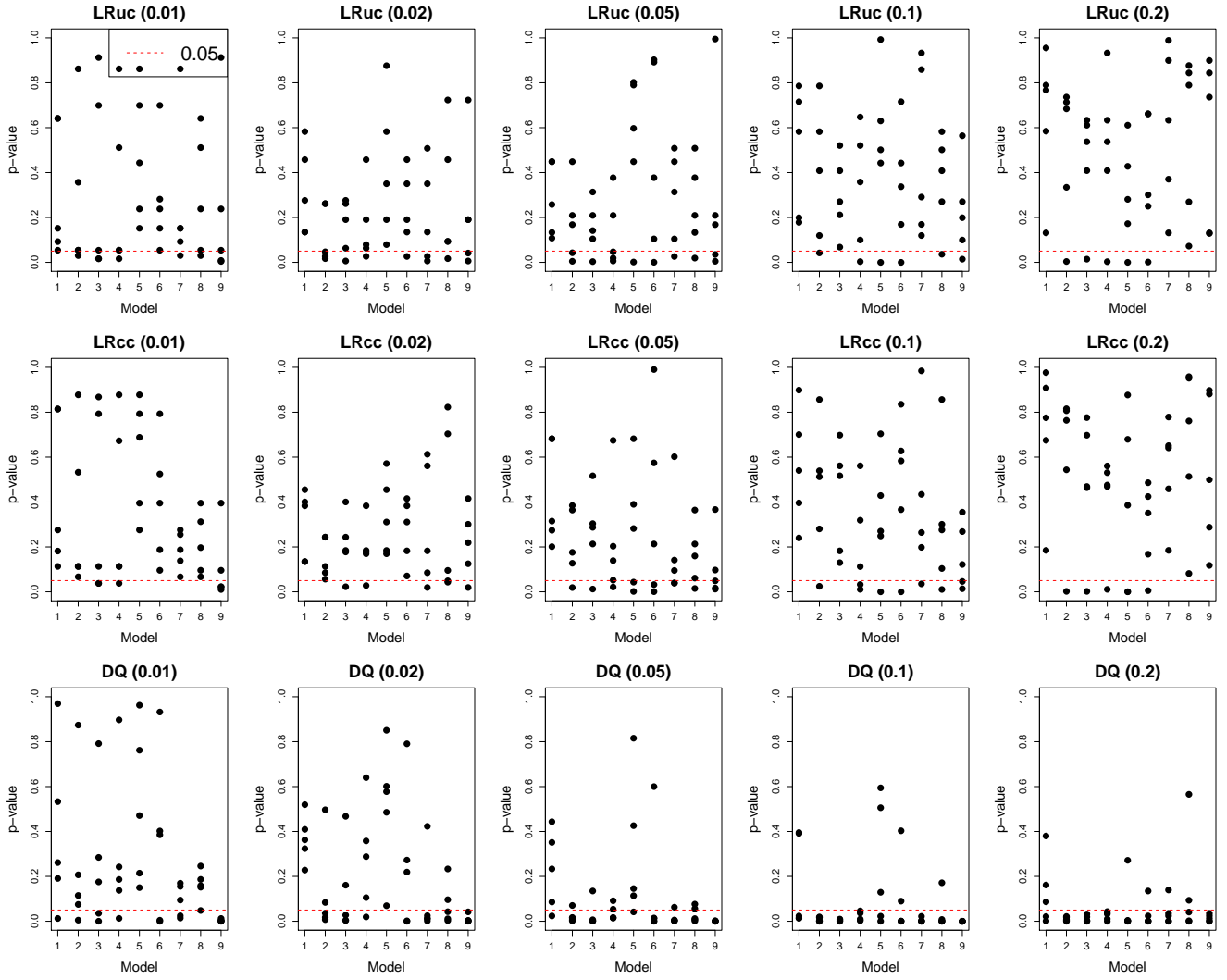


Figure B.2: Scatterplots for the p-values of LRuc, LRcc, and DQ tests with $q_0 = 0.01, 0.02, 0.05, 0.1, \text{ and } 0.2$. Note that the OGI (1), S-OGI (2), A-OGI (3), GJR-OGI (4), GJR (5), discrete GARCH (6), adjusted realized GARCH (7), adjusted HAR (8), and adjusted log-HAR (9).

(a) For $0 < \alpha_H < 1$ and $n \in \mathbb{N}$, we have

$$\int_{n-1}^{n-1+\lambda} \sigma_t^2(\theta) dt = \lambda h_n^H(\theta) + D_n^H \quad a.s.,$$

where

$$h_n^H(\theta) = \omega_H^g + \gamma h_{n-1}^H(\theta) + \alpha_H^g \lambda^{-1} \int_{n-2}^{n-2+\lambda} \sigma_t^2(\theta) dt + \beta_H^g (1 - \lambda)^{-1} (P_{n-1} - P_{n-2+\lambda})^2,$$

$$\begin{aligned}
\varrho_{H1} &= \alpha_H^{-1}(e^{\alpha_H} - 1), & \varrho_{H2} &= \alpha_H^{-2}(e^{\alpha_H} - 1 - \alpha_H), \\
\varrho_{H3} &= \alpha_H^{-3}(e^{\alpha_H} - 1 - \alpha_H - \alpha_H^2/2), & \varrho_H &= 2\gamma_H\varrho_{H3} + \varrho_{H1} - \varrho_{H2}, \\
\omega_H^g &= (1 - \gamma) [2\omega_{H1}\varrho_{H3} - \omega_{H2}\varrho_{H2} + \nu_H\{\varrho_{H2} - 2\varrho_{H3}\}] + \gamma_L(\omega_{H1} - \omega_{H2})\varrho_H + \omega_L\varrho_H, \\
\gamma &= \gamma_H\gamma_L, & \alpha_H^g &= \varrho_H\gamma_L\alpha_H, & \beta_H^g &= \varrho_H\beta_L + \beta_H(\varrho_{H2} - 2\varrho_{H3}),
\end{aligned}$$

and

$$D_n^H = 2\nu_H\alpha_H^{-2} \int_{n-1}^{n-1+\lambda} \{\alpha_H\lambda^{-1}(\lambda + n - 1 - t - \lambda\alpha_H^{-1})e^{\lambda^{-1}\alpha_H(\lambda+n-1-t)} + 1\} Z_t^H dW_t$$

is a martingale difference.

(b) For $0 < \beta_L < 1$, and $n \in \mathbb{N}$, we have

$$\int_{n-1+\lambda}^n \sigma_t^2(\theta) dt = (1 - \lambda)h_n^L(\theta) + D_n^L \quad a.s.,$$

where

$$h_n^L(\theta) = \omega_L^g + \gamma h_{n-1}^L(\theta) + \alpha_L^g \lambda^{-1} \int_{n-2}^{n-2+\lambda} \sigma_t^2(\theta) dt + \beta_L^g (1 - \lambda)^{-1} (P_{n-1} - P_{n-2+\lambda})^2,$$

$$\begin{aligned}
\varrho_{L1} &= \beta_L^{-1}(e^{\beta_L} - 1), & \varrho_{L2} &= \beta_L^{-2}(e^{\beta_L} - 1 - \beta_L), & \varrho_L &= (\gamma_L - 1)\varrho_{L2} + \varrho_{L1}, \\
\omega_L^g &= (1 - \gamma) [\omega_L\varrho_{L2} + \nu_L(\varrho_{L2} - 2\varrho_{L3})] + (\omega_{H1} - \omega_{H2} + \gamma_H\omega_L)\varrho_L + \varrho_L\alpha_H\omega_H^g \\
&+ \alpha_L(\varrho_{L2} - 2\varrho_{L3})\omega_H^g, & \alpha_L^g &= \varrho_L\alpha_H(\gamma + \alpha_H^g) + \alpha_L(\varrho_{L2} - 2\varrho_{L3})(\gamma + \alpha_H^g) \\
\beta_L^g &= \varrho_L(\gamma_H\beta_L + \alpha_H\beta_H^g) + \alpha_L(\varrho_{L2} - 2\varrho_{L3})\beta_H^g,
\end{aligned}$$

and

$$\begin{aligned}
D_n^L &= 2 \int_{n-1+\lambda}^n (e^{\beta_L(1-\lambda)^{-1}(n-t)} - 1)(P_t - P_{\lambda+n-1})\sigma_t(\theta)dB_t \\
&\quad + 2\nu_L\beta_L^{-2} \int_{n-1+\lambda}^n \left[\frac{\beta_L}{1-\lambda} \{n-t - (1-\lambda)\beta_L^{-1}\} e^{\beta_L(1-\lambda)^{-1}(n-t)} + 1 \right] Z_t^L dW_t \\
&\quad + (\varrho_L\beta_H + \alpha_L(\varrho_{L2} - 2\varrho_{L3}))(1-\lambda)\lambda^{-1}D_n^H
\end{aligned}$$

is a martingale difference.

(c) For $0 < \beta_H < 1$, $0 < \beta_L < 1$, and $n \in \mathbb{N}$, we have

$$\int_{n-1}^n \sigma_t^2(\theta)dt = h_n(\theta) + D_n \quad a.s.,$$

where $D_n = D_n^H + D_n^L$,

$$h_n(\theta) = \omega^g + \gamma h_{n-1}(\theta) + \alpha^g \lambda^{-1} \int_{n-2}^{n-2+\lambda} \sigma_t^2(\theta)dt + \beta^g (1-\lambda)^{-1} (P_{n-1} - P_{n-2+\lambda})^2, \quad (C.1)$$

$$\omega^g = \lambda\omega_H^g + (1-\lambda)\omega_L^g, \quad \alpha^g = \lambda\alpha_H^g + (1-\lambda)\gamma\alpha_L^g, \quad \beta^g = \lambda\beta_H^g + (1-\lambda)\beta_L^g.$$

(d) For $0 < \alpha_H < 1$, $0 < \beta_L < 1$, and $n \in \mathbb{N}$, we have

$$\begin{aligned}
E \left[\int_{n-1}^{n-1+\lambda} \sigma_t^2(\theta)dt \middle| \mathcal{F}_{n-1} \right] &= \lambda h_n^H(\theta) \quad a.s., \\
E \left[\int_{n-1+\lambda}^n \sigma_t^2(\theta)dt \middle| \mathcal{F}_{n-1} \right] &= (1-\lambda)h_n^L(\theta) \quad a.s., \\
E \left[\int_{n-1}^n \sigma_t^2(\theta)dt \middle| \mathcal{F}_{n-1} \right] &= h_n(\theta) \quad a.s.
\end{aligned}$$

Proof of Theorem C1. Consider (a) and (b). By Itô's lemma, we obtain

$$\begin{aligned}
R_H(k) &= \int_{n-1}^{\lambda+n-1} \frac{(\lambda+n-1-t)^k}{k!} \sigma_t^2(\theta) dt \\
&= \omega_{H1} 2\lambda^{-2} \frac{\lambda^{k+3}}{(k+3)!} - \omega_{H2} \lambda^{-1} \frac{\lambda^{k+2}}{(k+2)!} \\
&\quad + \sigma_{n-1}^2(\theta) \lambda^{-2} \left\{ \gamma_H 2 \frac{\lambda^{k+3}}{(k+3)!} - \lambda \frac{\lambda^{k+2}}{(k+2)!} + \lambda^2 \frac{\lambda^{k+1}}{(k+1)!} \right\} \\
&\quad + \frac{\beta_H}{\lambda^2(1-\lambda)} \left\{ \lambda \frac{\lambda^{k+2}}{(k+2)!} - 2 \frac{\lambda^{k+3}}{(k+3)!} \right\} \sum_{j=1}^{\infty} \gamma^{j-1} \left(\int_{n-1+\lambda-j}^{n-j} \sigma_s(\theta) dB_s \right)^2 \\
&\quad + \nu_H \lambda^{-2} \left\{ \lambda \frac{\lambda^{k+2}}{(k+2)!} - 2 \frac{\lambda^{k+3}}{(k+3)!} \right\} \\
&\quad + 2\lambda^{-2} \nu_H \int_{n-1}^{\lambda+n-1} \frac{(\lambda+n-1-s)^{k+2} (k+1)}{(k+2)!} (W_s - W_{n-1}) dW_s \\
&\quad + \alpha_H \lambda^{-1} R_H(k+1) \text{ a.s.}
\end{aligned}$$

Thus, we have

$$\begin{aligned}
R_H(0) &= \int_{n-1}^{\lambda+n-1} \sigma_t^2(\theta) dt \\
&= \lambda \sum_{k=0}^{\infty} \left(\omega_{H1} 2\alpha_H^{-3} \frac{\alpha_H^{k+3}}{(k+3)!} - \omega_{H2} \alpha_H^{-2} \frac{\alpha_H^{k+2}}{(k+2)!} \right) \\
&\quad + \sum_{k=0}^{\infty} \sigma_{n-1}^2(\theta) \lambda \left\{ \gamma_H 2\alpha_H^{-3} \frac{\alpha_H^{k+3}}{(k+3)!} - \alpha_H^{-2} \frac{\alpha_H^{k+2}}{(k+2)!} + \alpha_H^{-1} \frac{\alpha_H^{k+1}}{(k+1)!} \right\} \\
&\quad + \sum_{k=0}^{\infty} \frac{\beta_H}{(1-\lambda)} \lambda \left\{ \alpha_H^{-2} \frac{\alpha_H^{k+2}}{(k+2)!} - 2\alpha_H^{-3} \frac{\alpha_H^{k+3}}{(k+3)!} \right\} \sum_{j=1}^{\infty} \gamma^{j-1} \left(\int_{n-1+\lambda-j}^{n-j} \sigma_s(\theta) dB_s \right)^2 \\
&\quad + \sum_{k=0}^{\infty} \nu_H \lambda \left\{ \alpha_H^{-2} \frac{\alpha_H^{k+2}}{(k+2)!} - 2\alpha_H^{-3} \frac{\alpha_H^{k+3}}{(k+3)!} \right\} \\
&\quad + 2\nu_H \lambda^{-2} \sum_{k=0}^{\infty} \int_{n-1}^{\lambda+n-1} (\lambda^{-1} \alpha_H)^k \frac{(\lambda+n-1-t)^{k+2} (k+1)}{(k+2)!} Z_t^H dW_t \\
&= \lambda \omega_{H1} 2\varrho_{H3} - \lambda \omega_{H2} \varrho_{H2} + \nu_H \lambda \{ \varrho_{H2} - 2\varrho_{H3} \} \\
&\quad + \sigma_{n-1}^2(\theta) \lambda \{ 2\gamma_H \varrho_{H3} + \varrho_{H1} - \varrho_{H2} \} \\
&\quad + \lambda \frac{\beta_H}{(1-\lambda)} \{ \varrho_{H2} - 2\varrho_{H3} \} \sum_{j=1}^{\infty} \gamma^{j-1} \left(\int_{n-1+\lambda-j}^{n-j} \sigma_s(\theta) dB_s \right)^2 \\
&\quad + 2\nu_H \alpha_H^{-2} \int_{n-1}^{\lambda+n-1} \{ \alpha_H \lambda^{-1} (\lambda+n-1-t - \lambda \alpha_H^{-1}) e^{\lambda^{-1} \alpha_H (\lambda+n-1-t)} + 1 \} Z_t^H dW_t
\end{aligned}$$

$$= \lambda \left(\omega_H^g + \gamma h_{n-1}^H(\theta) + \alpha_H^g \lambda^{-1} \int_{n-2}^{\lambda+n-2} \sigma_t^2 dt + \beta_H^g (1-\lambda)^{-1} (P_{n-1} - P_{\lambda+n-2})^2 \right) + D_n^H \text{ a.s.}$$

Similarly, we have

$$\begin{aligned} R_L(k) &= \int_{\lambda+n-1}^n \frac{(n-t)^k}{k!} \sigma_t^2(\theta) dt \\ &= \omega_L (1-\lambda)^{-1} \frac{(1-\lambda)^{k+2}}{(k+2)!} + \sigma_{\lambda+n-1}^2(\theta) \left\{ \frac{\gamma_L - 1}{1-\lambda} \frac{(1-\lambda)^{k+2}}{(k+2)!} + \frac{(1-\lambda)^{k+1}}{(k+1)!} \right\} \\ &\quad + \nu_L (1-\lambda)^{-2} \left(\frac{(1-\lambda)^{k+3}}{(k+2)!} - 2 \frac{(1-\lambda)^{k+3}}{(k+3)!} \right) \\ &\quad + \frac{\alpha_L}{(1-\lambda)^2 \lambda} \left\{ (1-\lambda) \frac{(1-\lambda)^{k+2}}{(k+2)!} - 2 \frac{(1-\lambda)^{k+3}}{(k+3)!} \right\} \sum_{j=1}^{\infty} \gamma^{j-1} \int_{n-j}^{n-j+\lambda} \sigma_s^2(\theta) ds \\ &\quad + 2\nu_L (1-\lambda)^{-2} \int_{\lambda+n-1}^n \frac{(n-t)^{k+2} (k+1)}{(k+2)!} Z_t^L dW_t \\ &\quad + 2\beta_L (1-\lambda)^{-1} \int_{\lambda+n-1}^n \frac{(n-t)^{k+1}}{(k+1)!} (P_s - P_{\lambda+n-1}) \sigma_s(\theta) dB_s \\ &\quad + \beta_L (1-\lambda)^{-1} R_L(k+1) \text{ a.s.,} \end{aligned}$$

and

$$\begin{aligned} R_L(0) &= \int_{\lambda+n-1}^n \sigma_t^2(\theta) dt \\ &= (1-\lambda) \omega_L \varrho_{L2} + \nu_L (1-\lambda) (\varrho_{L2} - 2\varrho_{L3}) + \sigma_{\lambda+n-1}^2(\theta) (1-\lambda) \{ (\gamma_L - 1) \varrho_{L2} + \varrho_{L1} \} \\ &\quad + (1-\lambda) \frac{\alpha_L}{\lambda} \{ \varrho_{L2} - 2\varrho_{L3} \} \sum_{j=1}^{\infty} \gamma^{j-1} \int_{n-j}^{n-j+\lambda} \sigma_s^2(\theta) ds \\ &\quad + 2\nu_L \beta_L^{-2} \int_{\lambda+n-1}^n \left\{ \frac{\beta_L}{1-\lambda} (n-t - (1-\lambda) \beta_L^{-1}) e^{\beta_L (1-\lambda)^{-1} (n-t)} + 1 \right\} Z_t^L dW_t \\ &\quad + 2 \int_{\lambda+n-1}^n (e^{\beta_L (1-\lambda)^{-1} (n-t)} - 1) (P_t - P_{\lambda+n-1}) \sigma_t(\theta) dB_t \\ &= (1-\lambda) \left(\omega_L^g + \gamma h_{n-1}^L(\theta) + \alpha_L^g \lambda^{-1} \int_{n-2}^{\lambda+n-2} \sigma_t^2(\theta) dt + \beta_L^g (1-\lambda)^{-1} (P_{n-1} - P_{\lambda+n-2})^2 \right) \\ &\quad + D_n^L \text{ a.s.} \end{aligned}$$

The results of (c) and (d) are immediate consequences of (a) and (b). ■

Proof of Theorem C1 (b). To simplify the notations, we set $n = 1$. Simple algebraic

manipulations show

$$\begin{aligned}
E \left[(D_1^H)^2 \middle| \mathcal{F}_0 \right] &= 4\nu_H^2 \alpha_H^{-4} \int_0^\lambda t \{ \lambda^{-1} \alpha_H (\lambda - t - \alpha_H^{-1} \lambda) e^{\alpha_H \lambda^{-1} (\lambda - t)} + 1 \}^2 dt \\
&= \frac{\lambda^2 \nu_H^2 (2\alpha_H^2 - 8\alpha_H + 9) e^{2\alpha_H} + (16\alpha_H - 48) e^{\alpha_H} + 4\alpha_H^2 + 22\alpha_H + 39}{2\alpha_H^6} \\
&= \lambda^2 \nu_H^g,
\end{aligned}$$

where

$$\nu_H^g = \frac{2\alpha_H^6 \nu_H^2}{(2\alpha_H^2 - 8\alpha_H + 9) e^{2\alpha_H} + (16\alpha_H - 48) e^{\alpha_H} + 4\alpha_H^2 + 22\alpha_H + 39}. \quad (\text{C.2})$$

Consider D_n^{LL} . We first define

$$\begin{aligned}
f_{\beta_L,1}(t) &= \frac{3}{2} e^{\frac{6\beta_L}{1-\lambda}(1-t)} - \frac{1}{2} e^{\frac{2\beta_L}{1-\lambda}(1-t)}, \quad f_{\beta_L,2}(t) = \frac{1-\lambda}{\beta_L} (e^{\frac{\beta_L}{1-\lambda}(t-\lambda)} - 1), \\
f_{\beta_L,3}(t) &= \beta_L^{-2} [\{(\lambda-1)\beta_L - \lambda + 1\} e^{\frac{\beta_L}{1-\lambda}(t-\lambda)} - \{(t-1)\beta_L - \lambda + 1\}].
\end{aligned}$$

By Itô's Lemma, we obtain

$$\begin{aligned}
&E \left[\left(\int_\lambda^1 \left\{ \frac{\beta_L}{1-\lambda} (1-t - (1-\lambda)\beta_L^{-1}) e^{\beta_L(1-\lambda)^{-1}(1-t)} + 1 \right\} Z_t^L dW_t \right)^2 \right] \\
&E \left[\int_\lambda^1 \left\{ \frac{\beta_L}{1-\lambda} (1-t - (1-\lambda)\beta_L^{-1}) e^{\beta_L(1-\lambda)^{-1}(1-t)} + 1 \right\}^2 (t-\lambda) dt \right] \\
&= \frac{(1-\lambda)^2 ((2\beta_L^2 - 8\beta_L + 9) e^{2\beta_L} + (16\beta_L - 48) e^{\beta_L} + (4\beta_L^2 + 22\beta_L + 39))}{8\beta_L^2}
\end{aligned}$$

and

$$\begin{aligned}
&4E \left[\int_\lambda^1 e^{\frac{2\beta_L}{1-\lambda}(1-t)} (P_t - P_\lambda)^2 \sigma_t^2(\theta) dt \middle| \mathcal{F}_\lambda \right] \\
&= 4E \left[\int_\lambda^1 e^{\frac{2\beta_L}{1-\lambda}(1-t)} \left\{ \sigma_\lambda^2(\theta) + \frac{t-\lambda}{1-\lambda} (\omega_L + (\gamma_L - 1) \sigma_\lambda^2(\theta)) \right\} \int_\lambda^t \sigma_s^2(\theta) ds dt \middle| \mathcal{F}_\lambda \right]
\end{aligned}$$

$$\begin{aligned}
& +4E \left[\int_{\lambda}^1 e^{\frac{2\beta_L}{1-\lambda}(1-t)} \frac{\beta_L}{1-\lambda} (P_t - P_{\lambda})^4 dt \Big| \mathcal{F}_{\lambda} \right] \\
= & 4E \left[\int_{\lambda}^1 e^{\frac{2\beta_L}{1-\lambda}(1-t)} \left\{ \sigma_{\lambda}^2(\theta) + \frac{t-\lambda}{1-\lambda} (\omega_L + (\gamma_L - 1) \sigma_{\lambda}^2(\theta)) \right\} \int_{\lambda}^t \sigma_s^2(\theta) ds dt \Big| \mathcal{F}_{\lambda} \right] \\
& +12E \left[\int_{\lambda}^1 (e^{\frac{2\beta_L}{1-\lambda}(1-t)} - 1) (P_t - P_{\lambda})^2 \sigma_t^2(\theta) dt \Big| \mathcal{F}_{\lambda} \right] \text{ a.s.}
\end{aligned}$$

Thus, we have

$$\begin{aligned}
& E \left[\int_{\lambda}^1 e^{\frac{2\beta_L}{1-\lambda}(1-t)} (P_t - P_{\lambda})^2 \sigma_t^2(\theta) dt \Big| \mathcal{F}_{\lambda} \right] \\
= & \frac{3}{2} E \left[\int_{\lambda}^1 (P_t - P_{\lambda})^2 \sigma_t^2(\theta) dt \Big| \mathcal{F}_{\lambda} \right] \\
& - \frac{1}{2} E \left[\int_{\lambda}^1 e^{\frac{2\beta_L}{1-\lambda}(1-t)} \left\{ \sigma_{\lambda}^2(\theta) + \frac{t-\lambda}{1-\lambda} (\omega_L + (\gamma_L - 1) \sigma_{\lambda}^2(\theta)) \right\} \int_{\lambda}^t \sigma_s^2(\theta) ds dt \Big| \mathcal{F}_{\lambda} \right] \\
= & E \left[\int_{\lambda}^1 \left(\frac{3}{2} e^{\frac{6\beta_L}{1-\lambda}(1-t)} - \frac{1}{2} e^{\frac{2\beta_L}{1-\lambda}(1-t)} \right) \left\{ \sigma_{\lambda}^2(\theta) + \frac{t-\lambda}{1-\lambda} (\omega_L + (\gamma_L - 1) \sigma_{\lambda}^2(\theta)) \right\} \int_{\lambda}^t \sigma_s^2(\theta) ds dt \Big| \mathcal{F}_{\lambda} \right] \\
= & E \left[\int_{\lambda}^1 f_{\beta_L,1}(t) \left\{ \sigma_{\lambda}^2(\theta) + \frac{t-\lambda}{1-\lambda} (\omega_L + (\gamma_L - 1) \sigma_{\lambda}^2(\theta)) \right\} \right. \\
& \quad \left. \times \left\{ f_{\beta_L,2}(t) \sigma_{\lambda}^2(\theta) + f_{\beta_L,3}(t) (\omega_L + (\gamma_L - 1) \sigma_{\lambda}^2(\theta)) \right\} dt \Big| \mathcal{F}_{\lambda} \right] \\
= & \int_{\lambda}^1 \left(1 + \frac{t-\lambda}{1-\lambda} (\gamma_L - 1) \right) f_{\beta_L,1}(t) (f_{\beta_L,2}(t) + (\gamma_L - 1) f_{\beta_L,3}(t)) dt \sigma_{\lambda}^4(\theta) \\
& + \int_{\lambda}^1 \left[\left(1 + \frac{(t-\lambda)(\gamma_L - 1)}{1-\lambda} \right) f_{\beta_L,1}(t) f_{\beta_L,3}(t) \right. \\
& \quad \left. + \frac{(t-\lambda) f_{\beta_L,1}(t)}{1-\lambda} (f_{\beta_L,2}(t) + (\gamma_L - 1) f_{\beta_L,3}(t)) \right] dt \omega_L \sigma_{\lambda}^2(\theta) \\
& + \int_{\lambda}^1 \frac{t-\lambda}{1-\lambda} f_{\beta_L,1}(t) f_{\beta_L,3}(t) dt \omega_L^2 \\
= & \frac{1}{4} (F_{\beta_L,1} \sigma_{\lambda}^4(\theta) + F_{\beta_L,2} \omega_L \sigma_{\lambda}^2(\theta) + F_{\beta_L,3} \omega_L^2) \text{ a.s.},
\end{aligned}$$

where the second and third equalities are due to (C.4) and (C.5) below, respectively, and

$$\begin{aligned}
F_{\beta_L,1} &= 4 \int_{\lambda}^1 \left(1 + \frac{t-\lambda}{1-\lambda} (\gamma_L - 1) \right) f_{\beta_L,1}(t) (f_{\beta_L,2}(t) + (\gamma_L - 1) f_{\beta_L,3}(t)) dt, \\
F_{\beta_L,2} &= 4 \int_{\lambda}^1 \left[\left(1 + \frac{(t-\lambda)(\gamma_L - 1)}{1-\lambda} \right) f_{\beta_L,1}(t) f_{\beta_L,3}(t) \right. \\
& \quad \left. + \frac{(t-\lambda) f_{\beta_L,1}(t)}{1-\lambda} (f_{\beta_L,2}(t) + (\gamma_L - 1) f_{\beta_L,3}(t)) \right] dt
\end{aligned}$$

$$F_{\beta_L,3} = 4 \int_{\lambda}^1 \frac{t-\lambda}{1-\lambda} f_{\beta_L,1}(t) f_{\beta_L,3}(t) dt. \quad (C.3)$$

Hence, we arrive at

$$\begin{aligned} G(k) &= E \left[\int_{\lambda}^1 \frac{(1-t)^k}{k!} (P_t - P_{\lambda})^2 \sigma_t^2(\theta) dt \middle| \mathcal{F}_{\lambda} \right] \\ &= E \left[\int_{\lambda}^1 \frac{(1-t)^k}{k!} \left\{ \sigma_{\lambda}^2(\theta) + \frac{t-\lambda}{1-\lambda} (\omega_L + (\gamma_L - 1) \sigma_{\lambda}^2(\theta)) \right\} \int_{\lambda}^t \sigma_s^2(\theta) ds dt \middle| \mathcal{F}_{\lambda} \right] \\ &\quad + E \left[\int_{\lambda}^1 \frac{(1-t)^k}{k!} \frac{\beta_L}{1-\lambda} (P_t - P_{\lambda})^4 \middle| \mathcal{F}_{\lambda} \right] \\ &= E \left[\int_{\lambda}^1 \frac{(1-t)^k}{k!} \left\{ \sigma_{\lambda}^2(\theta) + \frac{t-\lambda}{1-\lambda} (\omega_L + (\gamma_L - 1) \sigma_{\lambda}^2(\theta)) \right\} \int_{\lambda}^t \sigma_s^2(\theta) ds dt \middle| \mathcal{F}_{\lambda} \right] \\ &\quad + \frac{6\beta_L}{1-\lambda} E \left[\int_{\lambda}^1 \frac{(1-t)^{k+1}}{(k+1)!} (P_t - P_{\lambda})^2 \sigma_t^2(\theta) dt \middle| \mathcal{F}_{\lambda} \right] \\ &= E \left[\int_{\lambda}^1 \frac{(1-t)^k}{k!} \left\{ \sigma_{\lambda}^2(\theta) + \frac{t-\lambda}{1-\lambda} (\omega_L + (\gamma_L - 1) \sigma_{\lambda}^2(\theta)) \right\} \int_{\lambda}^t \sigma_s^2(\theta) ds dt \middle| \mathcal{F}_{\lambda} \right] \\ &\quad + \frac{6\beta_L}{1-\lambda} G(k+1) \text{ a.s.}, \end{aligned}$$

where the second equality is due to Itô's Isometric, and the third equality can be derived using arguments similar to the proofs of Theorem ???. Therefore, we obtain

$$\begin{aligned} G(0) &= E \left[\int_{\lambda}^1 (P_t - P_{\lambda})^2 \sigma_t^2(\theta) dt \middle| \mathcal{F}_{\lambda} \right] \\ &= \sum_{k=0}^{\infty} (6\beta_L)^k E \left[\int_{\lambda}^1 \frac{(1-t)^k}{k!} \left\{ \sigma_{\lambda}^2(\theta) + \frac{t-\lambda}{1-\lambda} (\omega_L + (\gamma_L - 1) \sigma_{\lambda}^2(\theta)) \right\} \int_{\lambda}^t \sigma_s^2(\theta) ds dt \middle| \mathcal{F}_{\lambda} \right] \\ &= E \left[\int_{\lambda}^1 e^{\frac{6\beta_L}{1-\lambda}(1-t)} \left\{ \sigma_{\lambda}^2(\theta) + \frac{t-\lambda}{1-\lambda} (\omega_L + (\gamma_L - 1) \sigma_{\lambda}^2(\theta)) \right\} \int_{\lambda}^t \sigma_s^2(\theta) ds dt \middle| \mathcal{F}_{\lambda} \right] \text{ a.s.} \quad (C.4) \end{aligned}$$

Note that

$$\begin{aligned} &E \left[\int_{\lambda}^t \frac{(t-s)^k}{k!} \sigma_s^2(\theta) ds \middle| \mathcal{F}_{\lambda} \right] \\ &= E \left[\int_{\lambda}^t \frac{(t-s)^k}{k!} \left\{ \sigma_{\lambda}^2(\theta) + \frac{s-\lambda}{1-\lambda} (\omega_L + (\gamma_L - 1) \sigma_{\lambda}^2(\theta)) \right\} ds \middle| \mathcal{F}_{\lambda} \right] \end{aligned}$$

$$+ \frac{\beta_L}{1-\lambda} E \left[\int_{\lambda}^t \frac{(t-s)^{k+1}}{(k+1)!} \sigma_s^2(\theta) ds \middle| \mathcal{F}_{\lambda} \right] \text{ a.s.},$$

where the last equality can be derived similar to the proofs Theorem ???. We have

$$\begin{aligned} & E \left[\int_{\lambda}^t \sigma_s^2(\theta) ds \middle| \mathcal{F}_{\lambda} \right] \\ &= E \left[\int_{\lambda}^t e^{\frac{\beta_L}{1-\lambda}(t-s)} \left\{ \sigma_{\lambda}^2(\theta) + \frac{s-\lambda}{1-\lambda} (\omega_L + (\gamma_L - 1) \sigma_{\lambda}^2(\theta)) \right\} ds \middle| \mathcal{F}_{\lambda} \right] \\ &= f_{\beta_L,2}(t) \sigma_{\lambda}^2(\theta) + f_{\beta_L,3}(t) (\omega_L + (\gamma_L - 1) \sigma_{\lambda}^2(\theta)) \text{ a.s.}, \end{aligned} \tag{C.5}$$

and

$$\begin{aligned} & E \left[(D_1^{LL})^2 \middle| \mathcal{F}_{\lambda} \right] \\ &= F_{\beta_L,1} \sigma_{\lambda}^4(\theta) + F_{\beta_L,2} \omega_L \sigma_{\lambda}^2(\theta) + F_{\beta_L,3} \omega_L^2 + (1-\lambda)^2 \nu_L^g + (\alpha_L^* (1-\lambda) \lambda^{-1} D_1^H)^2 \\ &+ \frac{\nu_L^2 \left((2\beta_L^2 - 8\beta_L + 9) e^{2\beta_L} + (16\beta_L - 48) e^{\beta_L} + (4\beta_L^2 + 22\beta_L + 39) \right)}{2\beta_L^6} \text{ a.s.} \end{aligned}$$

Finally, an application of the tower property leads to

$$\begin{aligned} & E \left[(D_1^{LL})^2 \middle| \mathcal{F}_0 \right] \\ &= F_{\beta_L,1} s_0^4(\theta) + F_{\beta_L,2} \omega_L s_0^2(\theta) + F_{\beta_L,3} \omega_L^2 + (1-\lambda)^2 \nu_L^g \text{ a.s.}, \end{aligned}$$

where

$$s_0^2(\theta) = \omega_{H1} - \omega_{H2} + \gamma_H \omega_L + \gamma \sigma_{-1+\lambda}^2(\theta) + \beta_H h_1^H(\theta) + \frac{\gamma_H \beta_L}{1-\lambda} (X_n - X_{n-1+\lambda} - \int_{n-1+\lambda}^n \mu_t dt)^2, \tag{C.6}$$

$$\begin{aligned} \nu_L^g &= \frac{\nu_L^2 \left((2\beta_L^2 - 8\beta_L + 9) e^{2\beta_L} + (16\beta_L - 48) e^{\beta_L} + (4\beta_L^2 + 22\beta_L + 39) \right)}{2\beta_L^6} \\ &+ \{ (\varrho_L \beta_H (1-\lambda) \lambda^{-1})^2 + (\beta_H \lambda^{-1})^2 \} \nu_H^g. \end{aligned} \tag{C.7}$$

■

C.2 Proof of Theorem ??

To easy the notations, we use θ instead of θ^g in this subsection. Define

$$\begin{aligned}\widehat{L}_{n,m}(\theta) &= -\frac{1}{n} \sum_{i=1}^n \left[\frac{(RV_i - \lambda \widehat{h}_i^H(\theta))^2}{\widehat{\phi}_H} + \frac{((X_i - X_{\lambda+i-1})^2 - (1-\lambda)\widehat{h}_i^L(\theta))^2}{\widehat{\phi}_L} \right], \\ \widehat{L}_n(\theta, \phi_H, \phi_L) &= -\frac{1}{n} \sum_{i=1}^n \left[\frac{(IV_i - \lambda h_i^H(\theta))^2}{\phi_H} + \frac{((X_i - X_{\lambda+i-1})^2 - (1-\lambda)h_i^L(\theta))^2}{\phi_L} \right], \\ L_n(\theta) &= -\frac{1}{n} \sum_{i=1}^n \left[\frac{\lambda^2 (h_i^H(\theta_0) - h_i^H(\theta))^2 + \varphi^H(\theta_0)}{\phi_{H0}} + \frac{(1-\lambda)^2 (h_i^L(\theta_0) - h_i^L(\theta))^2 + \varphi_i^L(\theta_0)}{\phi_{H0}} \right], \\ \widehat{s}_{n,m}(\theta) &= \frac{\partial \widehat{L}_{n,m}(\theta)}{\partial \theta}, \widehat{s}_n(\theta, \phi_H, \phi_L) = \frac{\partial \widehat{L}_n(\theta, \phi_H, \phi_L)}{\partial \theta}, s_n(\theta) = \frac{\partial L_n(\theta)}{\partial \theta},\end{aligned}$$

where $IV_i = \int_{i-1}^{\lambda+i-1} \sigma_t^2(\theta_0) dt$. Since the effect of the initial value $h_1(\theta)$ is of order n^{-1} and thus negligible, without loss of the generality, we assume $h_1(\theta_0)$ is given.

Proposition C1. *Under the assumption of Theorem ??, $\widehat{\theta}$ converges to θ_0 in probability.*

Proof of Proposition C1. Note that

$$|\widehat{L}_{n,m}(\theta) - L_n(\theta)| \leq |\widehat{L}_{n,m}(\theta) - \widehat{L}_n(\theta, \theta_0)| + |\widehat{L}_n(\theta, \theta_0) - L_n(\theta)|.$$

First consider $|\widehat{L}_{n,m}(\theta) - \widehat{L}_n(\theta, \theta_0)|$. By Assumption ??(4), we have

$$\begin{aligned}E \left[\sup_{\theta} |\widehat{h}_i^H(\theta) - h_i^H(\theta)| \right] &\leq C \sum_{k=0}^{i-2} \gamma_u^k E(|RV_{i-1-k} - IV_{i-1-k}|) \\ &\leq Cm^{-1/4},\end{aligned}\tag{C.8}$$

and similarly, we can show

$$E \left[\sup_{\theta} |\widehat{h}_i^L(\theta) - h_i^L(\theta)| \right] \leq Cm^{-1/4}.\tag{C.9}$$

Together with Assumption ??(6), we obtain

$$\sup_{\theta \in \Theta} |\widehat{L}_{n,m}(\theta) - \widehat{L}_n(\theta, \theta_0)| = o_p(1).$$

Consider the second term $|\widehat{L}_n(\theta, \theta_0) - L_n(\theta)|$. We have

$$\begin{aligned} & \widehat{L}_n(\theta, \theta_0) - L_n(\theta) \\ &= -\frac{1}{n} \sum_{i=1}^n \left[\frac{\lambda D_i^H (h_i^H(\theta_0) - h_i^H(\theta)) + (D_i^H)^2 - \varphi^H(\theta_0)}{\phi_{H0}} \right. \\ & \quad \left. + \frac{D_i^{LL} (1 - \lambda) \{h_i^L(\theta_0) - h_i^L(\theta)\} + (D_i^{LL})^2 - \varphi_i^L(\theta_0)}{\phi_{L0}} \right]. \end{aligned}$$

Note that the martingale difference terms, D_i^H and D_i^{LL} , are integrable. The uniform convergence of the second term $|\widehat{L}_n(\theta, \theta_0) - L_n(\theta)|$ can be established using arguments similar to the proofs of Theorem 1 in Kim and Wang (2016). Then, to prove the statement, we need to show the uniqueness of the maximizer of $L_n(\theta)$. $L_n(\theta)$ is concave, and the solution of the equation with its first derivative equal to zero must satisfy $h_i^H(\theta) = h_i^H(\theta_0)$ and $h_i^L(\theta) = h_i^L(\theta_0)$ for all $i = 1, \dots, n$. Thus, the maximizer θ^* must satisfy $h_i^H(\theta^*) = h_i^H(\theta_0)$ and $h_i^L(\theta^*) = h_i^L(\theta_0)$ for all $i = 1, \dots, n$. Suppose that the maximizer θ^* may be different from θ_0 . Since

$$h_i^H(\theta) = \omega_H^g + \gamma h_{i-1}^H(\theta) + \frac{\alpha_H^g}{\lambda} IV_{i-1} + \frac{\beta_H^g}{1 - \lambda} (X_{i-1} - X_{\lambda+i-2})^2,$$

θ^* and θ_0 satisfy almost surely

$$\mathbf{T} \begin{pmatrix} \omega_{H,0}^g - \omega_H^* \\ \gamma_0 - \gamma^* \\ \beta_{H,0}^g - \beta_H^* \\ \alpha_{H,0}^g - \alpha_H^* \end{pmatrix} = 0,$$

where

$$\mathbf{T} = \begin{pmatrix} 1 & h_1^H(\theta_0) & (X_1 - X_\lambda)^2 & IV_1 \\ 1 & h_2^H(\theta_0) & (X_2 - X_{\lambda+1})^2 & IV_2 \\ \vdots & \vdots & \vdots & \vdots \\ 1 & h_n^H(\theta_0) & (X_{n-1} - X_{\lambda+n-1})^2 & IV_{n-1} \end{pmatrix}.$$

Then, since IV_i 's and X_i 's are nondegenerate random variables, we have

$$\begin{pmatrix} \omega_{H,0}^g - \omega_H^* \\ \gamma_0 - \gamma^* \\ \beta_{H,0}^g - \beta_H^* \\ \alpha_{H,0}^g - \alpha_H^* \end{pmatrix} = 0 \text{ a.s.},$$

and similarly, we obtain

$$\begin{pmatrix} \omega_{L,0}^g - \omega_L^* \\ \gamma_0 - \gamma^* \\ \beta_{L,0}^g - \beta_L^* \\ \alpha_{L,0}^g - \alpha_L^* \end{pmatrix} = 0 \text{ a.s.},$$

which implies $\theta^* = \theta_0$ a.s. This shows that the maximizer is unique. Finally, the result is a consequence of Theorem 1 in Xiu (2010). ■

Proof of Theorem ??. The mean value theorem and Taylor expansion indicate that for some θ^* between θ_0 and $\hat{\theta}$, we have

$$\hat{s}_{n,m}(\hat{\theta}) - \hat{s}_{n,m}(\theta_0) = -\hat{s}_{n,m}(\theta_0) = -\nabla \hat{s}_{n,m}(\theta^*)(\hat{\theta} - \theta_0).$$

By Theorem ??, we have

$$\begin{pmatrix} h_n^H(\theta_0) \\ h_n^L(\theta_0) \end{pmatrix} = \begin{pmatrix} \gamma_0 + \frac{\alpha_{H,0}^g}{\lambda} & \frac{\beta_{H,0}^g}{1-\lambda} \\ \frac{\alpha_{L,0}^g}{\lambda} & \gamma_0 + \frac{\beta_{L,0}^g}{1-\lambda} \end{pmatrix} \begin{pmatrix} h_{n-1}^H(\theta_0) \\ h_{n-1}^L(\theta_0) \end{pmatrix} + \begin{pmatrix} \omega_{H,0}^g + \frac{\alpha_{H,0}^g}{\lambda} D_{n-1}^H + \frac{\beta_{H,0}^g}{1-\lambda} D_{n-1}^{LL} \\ \omega_{L,0}^g + \frac{\alpha_{L,0}^g}{\lambda} D_{n-1}^H + \frac{\beta_{L,0}^g}{1-\lambda} D_{n-1}^{LL} \end{pmatrix}.$$

Thus, by Assumption ?? (1) and (5), $h_n^H(\theta_0)$ and $h_n^L(\theta_0)$ are stationary. Since $(X_n - X_{\lambda+n-1})^2$ and IV_n are functions of $h_n^H(\theta_0)$, $h_n^L(\theta_0)$, D_n^H and D_n^{LL} , $(X_n - X_{\lambda+n-1})^2$ and IV_n are stationary. Then, similar to the proofs of Proposition C1, we can show

$$-\nabla \widehat{s}_{n,m}(\theta^*) \xrightarrow{p} -\nabla s_n(\theta_0).$$

Since IV_i 's and X_i 's are nondegenerate, $-\nabla s_n(\theta_0)$ is almost surely positive definite. By the ergodic theorem, we have

$$-\nabla s_n(\theta_0) \xrightarrow{p} 2A.$$

Thus, we obtain

$$|\widehat{s}_{n,m}(\theta_0) - \widehat{s}_n(\theta_0, \phi_{H0}, \phi_{L0})| \leq |\widehat{s}_{n,m}(\theta_0) - \widehat{s}_n(\theta_0, \widehat{\phi}_H, \widehat{\phi}_L)| + |\widehat{s}_n(\theta_0, \widehat{\phi}_H, \widehat{\phi}_L) - \widehat{s}_n(\theta_0, \phi_{H0}, \phi_{L0})|.$$

By Assumption ?? and (C.8)–(C.9), we can establish

$$|\widehat{s}_{n,m}(\theta_0) - \widehat{s}_n(\theta_0, \widehat{\phi}_H, \widehat{\phi}_L)| = O_p(m^{-1/4}). \quad (\text{C.10})$$

Consider $|\widehat{s}_n(\theta_0, \widehat{\phi}_H, \widehat{\phi}_L) - \widehat{s}_n(\theta_0, \phi_{H0}, \phi_{L0})|$. Simple algebraic manipulations show

$$\begin{aligned} \widehat{s}_n(\theta_0, \widehat{\phi}_H, \widehat{\phi}_L) - \widehat{s}_n(\theta_0, \phi_{H0}, \phi_{L0}) &= \frac{1}{n} \sum_{i=1}^n 2\lambda D_i^H \frac{\partial h_i^H(\theta_0)}{\partial \theta} \left(\frac{1}{\widehat{\phi}_H} - \frac{1}{\phi_H} \right) \\ &\quad + 2(1-\lambda) D_i^{LL} \frac{\partial h_i^L(\theta_0)}{\partial \theta} \left(\frac{1}{\widehat{\phi}_L} - \frac{1}{\phi_L} \right). \end{aligned}$$

Since D_i^H 's are martingale differences and $h_i^H(\theta_0)$ is \mathcal{F}_{i-1} -adaptive, we have $\frac{2\lambda}{n} \sum_{i=1}^n D_i^H \frac{\partial h_i^H(\theta_0)}{\partial \theta} = O_p(n^{1/2})$. Thus, with $\|\widehat{\phi}_H - \phi_{H0}\|_{\max} = o_p(1)$, we obtain

$$\frac{1}{n} \sum_{i=1}^n 2\lambda D_i^H \frac{\partial h_i^H(\theta_0)}{\partial \theta} \left(\frac{1}{\varphi^H(\widehat{\theta}_1)} - \frac{1}{\varphi^H(\theta_0)} \right) = o_p(n^{-1/2}).$$

Similarly, we can show

$$\frac{1}{n} \sum_{i=1}^n D_i^{LL} \frac{\partial h_i^L(\theta_0)}{\partial \theta} \left(\frac{1}{\widehat{\phi}_L} - \frac{1}{\phi_L} \right) = o_p(n^{-1/2}).$$

Hence, we have

$$\widehat{s}_n(\theta_0, \widehat{\phi}_H, \widehat{\phi}_L) - \widehat{s}_n(\theta_0, \phi_{H0}, \phi_{L0}) = o_p(n^{-1/2}). \quad (\text{C.11})$$

By (C.10) and (C.11), we obtain

$$|\widehat{s}_{n,m}(\theta_0) - \widehat{s}_n(\theta_0, \phi_{H0}, \phi_{L0})| = O_p(m^{-1/4}) + o_p(n^{-1/2}).$$

Note that

$$\widehat{s}_n(\theta_0, \phi_{H0}, \phi_{L0}) = \frac{1}{n} \sum_{i=1}^n 2\lambda \frac{D_i^H}{\phi_{H0}} \frac{\partial h_i^H(\theta_0)}{\partial \theta} + 2(1-\lambda) \frac{D_i^{LL}}{\phi_{L0}} \frac{\partial h_i^L(\theta_0)}{\partial \theta}.$$

Since the martingale difference terms have the finite 4th moments, the above term convergence rate is $n^{-1/2}$. Thus, (??) is proved. An application of the ergodic theorem leads to

$$\sqrt{n} \widehat{s}_n(\theta_0) \xrightarrow{d} N(0, 4B).$$

Finally, we conclude

$$\begin{aligned}\sqrt{n}(\widehat{\theta} - \theta_0) &= -\frac{1}{2}A^{-1}\sqrt{n}\widehat{s}_n(\theta_0) + o_p(1) \\ &\xrightarrow{d} N(0, A^{-1}BA^{-1}).\end{aligned}$$

The statement (??) is proved. ■

References

- Aït-Sahalia, Y. and Xiu, D. (2016). Increased correlation among asset classes: Are volatility or jumps to blame, or both? *Journal of Econometrics*, 194(2):205–219.
- Jacod, J., Li, Y., Mykland, P. A., Podolskij, M., and Vetter, M. (2009). Microstructure noise in the continuous case: the pre-averaging approach. *Stochastic processes and their applications*, 119(7):2249–2276.
- Kim, D. and Wang, Y. (2016). Unified discrete-time and continuous-time models and statistical inferences for merged low-frequency and high-frequency financial data. *Journal of Econometrics*, 194:220–230.
- Xiu, D. (2010). Quasi-maximum likelihood estimation of volatility with high frequency data. *Journal of Econometrics*, 159(1):235–250.